

# Establishing the Primary HEFT as a Precision Benchmark for UV-HEFT Matching

Zizhou Ge\* and Xia Wan†

*School of physics and Information Technology,*

*Shaanxi Normal University, Xi'an 710119, China*

Huayang Song‡

*Particle Theory and Cosmology Group,*

*Center for Theoretical Physics of the Universe,*

*Institute for Basic Science (IBS), Daejeon, 34126, Korea*

(Dated: February 17, 2026)

## Abstract

We match the real Higgs triplet model (RHTM) onto HEFT under different parameter choices and power-counting schemes, thereby obtaining several representative HEFT formulations and clarifying their relations. We establish the primary HEFT (pHEFT) as a benchmark framework, demonstrating that alternative HEFT constructions can be systematically derived from it. A key advantage of the pHEFT construction is its parameter choice, which maintains linear relations between the UV Lagrangian parameters and squared heavy masses. By strictly employing the inverse squared heavy masses as the expansion parameters without imposing additional constraints, pHEFT preserves maximal ultraviolet (UV) information and ensures higher perturbative accuracy by avoiding the additional truncations inherent in more complex, non-linear formulations or extra constraints. Through the analysis of the  $Z_2$ -symmetric real singlet model and the 2HDM, we illustrate the criteria for identifying viable primary HEFT constructions in UV models with scalar extensions. Furthermore, for the first time, we derive the HEFT operators of the RHTM involving fermions.

## CONTENTS

|   |    |
|---|----|
| I. Introduction   | 3  |
| II. HEFT and the model  | 7  |
| A. HEFT   | 7  |
| B. The Real Higgs Triplet Model (RHTM)                                  | 8  |
| 1. The model in a non-linear representation                             | 8  |
| 2. Linear Relations Between Squared Masses and UV Lagrangian Parameters | 9  |
| III. HEFTs of the RHTM  | 10 |
| A. Primary HEFT and decoupling HEFT                                     | 10 |
| 1. Parameter Set  | 10 |
| 2. Power Countings  | 11 |
| 3. The matching results   | 12 |
| 4. The mapping from pHEFT to dHEFT                                      | 15 |

---

<sup>\*</sup> The authors are listed in alphabetical order by last name.; [gezizhou@snnu.edu.cn](mailto:gezizhou@snnu.edu.cn)

<sup>†</sup> [wanxia@snnu.edu.cn](mailto:wanxia@snnu.edu.cn)

<sup>‡</sup> [huayangs1990@ibs.re.kr](mailto:huayangs1990@ibs.re.kr)

|   |    |
|---|----|
| 5. Discussion on Framework Correspondence                             | 18 |
| B. $Z_2$ -HEFT  | 22 |
| C. $\xi$ -HEFT  | 27 |
| D. $Y_2$ -HEFT vs. SMEFT  | 30 |
| 1. $Y_2$ -HEFT  | 30 |
| 2. SMEFT  | 31 |
| IV. The Primary HEFT of other UV Models                               | 32 |
| A. Z2RSM  | 33 |
| 1. Model Setup and Parameterization                                   | 33 |
| 2. Construction of the primary HEFT: parameter set and power counting | 34 |
| B. 2HDM   | 35 |
| 1. General Basis vs. Higgs Basis                                      | 35 |
| 2. Construction of the primary HEFT: parameter set and power counting | 36 |
| V. Conclusion and Discussion  | 38 |
| A. Solutions for the Heavy Fields in the pHEFT                        | 40 |
| B. EoM of $U$   | 41 |
| Acknowledgments   | 42 |
| References  | 42 |

## I. INTRODUCTION

Since the Higgs boson is discovered at the Large Hadron Collider (LHC) [1, 2], looking for new physics beyond the Standard Model (BSM) at the LHC becomes the predominant goal of high energy physics. Although experimental measurements have become increasingly precise, there is no clear evidence for the existence of BSM particles [3, 4]. This suggests that new physics, if it exists, is likely to reside at a higher energy scale, such as the TeV scale. Effective field theories (EFTs) formulated at the electroweak scale, extending the SM, provide a systematic framework for parameterizing new-physics effects [5, 6].

At the electroweak energy scale, two main types of Effective Field Theories (EFTs) are used: Standard Model EFT (SMEFT) [7–10] and Higgs EFT (HEFT) [11–33]. Both SMEFT and HEFT include the same particle content as the SM. Their difference fundamentally stems from the assumption about the symmetry realization of the Higgs boson. In SMEFT, the Higgs and the three Goldstones together form a  $SU(2)_L$  doublet as in the SM. HEFT treats the Higgs as an  $SU(2)_L$  singlet with non-linearly transforming Goldstones, and encompasses the SMEFT doublet description as a special limiting case [25, 27, 34]. Over the past decade, the SMEFT has gained popularity and developed rapidly [35–43], partly due to its linear structure, which allows for a concise formulation. Nevertheless, the SMEFT framework is not always adequate. When new physics introduces additional sources of electroweak symmetry breaking or involves non-decoupling heavy degrees of freedom [44, 45], the effects of new physics cannot be consistently captured within the SMEFT framework and require a HEFT description. There has been a notable increase in research on HEFT in recent years [32, 33, 46–61].

EFTs can be useful purely from the bottom up: one specifies the physical degrees of freedom along with their transformations under a certain set of symmetries and identifies a power counting scheme to organize the operator expansion. Though in this sense EFTs are “model independent” and as such they provide an approach for classifying observables which deviate from the SM predictions, the top down approach is more useful to help understanding the (more) fundamental ultraviolet (UV) description of nature. In this scenario, a certain BSM model is assumed, and a process, known as “matching”, is carried out between the EFTs and the UV model by “integrating out” the “heavy” degrees of freedom. However, it should be noted that the expansion parameter used during matching is generally method-dependent and can differ from the power-counting parameter used in the bottom-up approach.

Within BSM physics, commonly used matching methods are performing the heavy mass expansion via either diagrammatic calculation or functional prescription [41, 62, 63]. This exercise has been done especially for the SMEFT but also the HEFT, considering several different UV models [64–67]. Following this direction, several automatic matching tools are developed [68–71]. However, even for the SMEFT, such expansion parameters (the inverse powers of the BSM state masses) are not fully consistent with the SMEFT metric (canonical dimension): 1) due to computational limitations, we must perform a truncated loop expansion implicitly in the above description; 2) the extra dimensional parameters  $\mu_i$  in the UV

theory can give potential corrections, which are generally also incalculable in full, at the order of  $\mu_i^n/M_j^{d+n-4}$  to the  $d$ -dim operators. This discrepancy between the power counting and the matching expansion parameter becomes more evident in HEFT, since its operator expansion is organized by chiral dimension. Without other known mathematical tools, we must rely on this approach, expanding the propagators of the heavy BSM states order by order <sup>1</sup> <sup>2</sup>. Therefore, top-down matching essentially fixes the parametric scaling of the Wilson coefficients <sup>3</sup>. After electroweak symmetry breaking, the lifting of degeneracies in the BSM spectrum leads to a richer structure in the UV-HEFT matching. Further the inclusion of experimental constraints renders the power-counting scheme non-unique [72] (see Sec. III for concrete examples). It is therefore worthwhile to study the relations among different HEFTs from the same UV completion, with the aim of providing practical guidance for phenomenological applications. A central challenge in this endeavor is whether a consistent and practically useful power-counting scheme can be formulated for UV-HEFT matching, especially one that is amenable to automation, since any systematic use of HEFT ultimately relies on automated tools.

In this work, we find that in new physics models with scalar extensions, there exists such a HEFT, named the primary HEFT, that can play this role. Starting from a UV parameter set consisting of heavy masses, mixing angles, and VEVs, we adopt a power-counting scheme that expands in inverse powers of heavy masses and organizes operators accordingly, without imposing additional restrictions. This matching procedure preserves maximal information within the specified expansion order. Other HEFTs can thus be mapped from this primary HEFT by imposing further restrictions or performing parameter transformations.

---

<sup>1</sup> Though physicists usually say that there are two matching methods, diagrammatic and functional methods, the physics behind them are same, that propagators of the BSM states are introduced and shrunk to some contacted interactions.

<sup>2</sup> One could imagine that a lattice simulation matching, like what is done in the matching between QCD and chiral perturbation theory, can in principle be performed to obtain the HEFT's Wilson coefficients without introducing a different power counting parameter besides the chiral dimension. However, due to the technical obstacles to simulating chiral fermions on the lattice and also the resource consumption, a systematic study of the lattice matching between generic UV theories and HEFT is, to our knowledge, still lacking.

<sup>3</sup> We will employ the term “power-counting scheme” in a flexible manner to encompass both related concepts, relying on the sentence context to clarify the specific meaning.

The accuracy of an EFT is fundamentally determined by the convergence of its power-counting expansion. In this context, the primary HEFT achieves superior accuracy at a specific order (e.g.,  $1/M^n$ ) because it encapsulates the complete UV dynamics without the loss of information incurred by additional parametric simplifications. While restricted HEFTs may be easier to implement for specific phenomenological studies, they often neglect sub-leading mixing effects, or assume specific hierarchies between VEVs to justify further truncations, thereby leading to a loss of fidelity relative to the UV theory. By utilizing the primary HEFT as a benchmark, the truncation error introduced by these further approximations can be quantified, ensuring a controlled and systematic mapping from the primary HEFT to other HEFTs.

Using the real Higgs triplet model (RHTM) as an explicit example, we construct its primary HEFT and several alternative HEFT descriptions. Compared with the primary HEFT, these alternative HEFTs differ from the primary HEFT either by adopting different scaling behaviors for the same parameter set, or by employing different parameter sets that may or may not explicitly include heavy mass parameters, leading to intrinsically different power-counting schemes. By studying the mappings from the primary HEFT to these alternative HEFTs, we demonstrate how accuracy is progressively lost under different power-counting schemes and their associated truncations. We further present numerical comparisons for the  $hh \rightarrow hh$  scattering process to illustrate these effects quantitatively.

In addition, by mapping the primary HEFT onto a specific parameter space that mimics the SMEFT setting, we obtain a formulation that recovers the SMEFT results at the amplitude level. The exact agreement found in our calculation suggests that, under this mapping, the HEFT becomes phenomenologically equivalent to the SMEFT (after spontaneous symmetry breaking) across a general class of processes.

The paper is organized as follows: In Sec. II we introduce the HEFT formulation and the RHTM. Sec. III include five parts. In Sec. III A we first obtain the primary HEFT(pHEFT) and decoupling HEFT(dHEFT) of RHTM, then get their mapping relation and discuss their correspondence. In Sec. III B, we introduce the  $Z_2$ -HEFT and point out that a viable primary HEFT requires a parameterization in which the UV Lagrangian parameters is polynomial to the squared heavy masses. In Sec. III C, We establish a hierarchical relation among the pHEFT, dHEFT and  $\xi$ -HEFT. In Sec. III D, based on the SMEFT parameter set and power-counting scheme, we map the pHEFT to the  $Y_2$ -HEFT and reproduce the SMEFT

predictions. In Sec. IV we introduce the good primary HEFT for Z2RSM and 2HDM. Sec. V gives a discuss and conclusion.

## II. HEFT AND THE MODEL

### A. HEFT

The Higgs sector in the SM has an approximate global symmetry  $SU(2)_L \times SU(2)_R$  which is spontaneously broken down to the custodial symmetry  $SU(2)_C$  by the Higgs vacuum expectation value (VEV). Using the CCWZ formalism [73], one can build an EFT, known as the HEFT, describing the interactions of the non-linearly realized Goldstone bosons among themselves and with other SM fields, where a real scalar denotes the Higgs field. The Goldstones  $\pi_i$  are usually treated as a single object, a unitary matrix  $U \equiv \exp\left(\frac{i\pi_i\sigma_i}{v_{\text{EW}}}\right)$ , where  $\sigma_i$  are the three Pauli matrices. At the lowest order, the HEFT Lagrangian reads<sup>4</sup>

$$\begin{aligned} \mathcal{L}_{\text{HEFT}}^{\text{LO}} \supset & \frac{1}{2}\partial_\mu h\partial^\mu h - \mathcal{V}(h) + \frac{v_{\text{EW}}^2}{4}\mathcal{F}(h)\langle D_\mu U^\dagger D^\mu U \rangle \\ & + \frac{v_{\text{EW}}^2}{4}\mathcal{G}(h)\langle U^\dagger D_\mu U\sigma_3 \rangle\langle U^\dagger D^\mu U\sigma_3 \rangle \\ & - \frac{v_{\text{EW}}}{\sqrt{2}}\left(\bar{Q}_L U \mathcal{Y}_Q(h) Q_R + \bar{L}_L U \mathcal{Y}_L(h) L_R + \text{h.c.}\right), \end{aligned} \quad (1)$$

where  $v_{\text{EW}} = 246 \text{ GeV}$  represents the electroweak VEV,  $\langle \cdots \rangle$  denotes the trace,  $D_\mu$  is the covariant derivative, and  $\mathcal{V}(h)$ ,  $\mathcal{F}(h)$ ,  $\mathcal{G}(h)$ , and  $\mathcal{Y}_{Q/L}(h)$  are polynomial functions of  $h$  with the following forms,

$$\mathcal{V}(h) = \frac{1}{2}m_h^2 h^2 \left[ 1 + (1 + \Delta\kappa_3)\frac{h}{v_{\text{EW}}} + \frac{1}{4}(1 + \Delta\kappa_4)\frac{h^2}{v_{\text{EW}}^2} + \cdots \right], \quad (2)$$

$$\mathcal{F}(h) = 1 + 2(1 + \Delta a)\frac{h}{v_{\text{EW}}} + (1 + \Delta b)\frac{h^2}{v_{\text{EW}}^2} + \cdots, \quad (3)$$

$$\mathcal{G}(h) = \Delta\alpha + \Delta a^\phi\frac{h}{v_{\text{EW}}} + \Delta b^\phi\frac{h^2}{v_{\text{EW}}^2} + \cdots, \quad (4)$$

$$\mathcal{Y}_Q(h) = \text{diag}\left(\sum_n Y_U^{(n)}\frac{h^n}{v_{\text{EW}}^n}, \sum_n Y_D^{(n)}\frac{h^n}{v_{\text{EW}}^n}\right), \quad \mathcal{Y}_L(h) = \text{diag}\left(0, \sum_n Y_\ell^{(n)}\frac{h^n}{v_{\text{EW}}^n}\right). \quad (5)$$

The first term is the Higgs potential. The second and third terms describe the Goldstones dynamic term which contains the gauge boson mass terms and interactions between Higgs

---

<sup>4</sup> Only terms relevant for our purposes are shown. The kinetic terms for gauge bosons and fermions are omitted.

and massive gauge bosons; and note that the third one breaks the custodial symmetry. The four term generates fermion masses and Higgs-fermion interactions.

## B. The Real Higgs Triplet Model (RHTM)

### 1. The model in a non-linear representation

In the RHTM besides the  $SU(2)_L$  doublet there exists a triplet with hyper-charge  $Y = 0$ . The Lagrangian of RHTM can be expressed as [62, 63, 74, 75] (for phenomenological studies, cf. e.g. Refs. [76–79])

$$\begin{aligned}\mathcal{L} &\supset (D_\mu H)^\dagger (D^\mu H) + \langle D_\mu \Sigma^\dagger D^\mu \Sigma \rangle - V_S - V_Q, \\ V_S &= Y_1^2 H^\dagger H + Z_1 (H^\dagger H)^2 + Y_2^2 \langle \Sigma^\dagger \Sigma \rangle + Z_2 \langle \Sigma^\dagger \Sigma \rangle^2 + Z_3 H^\dagger H \langle \Sigma^\dagger \Sigma \rangle + 2Y_3 H^\dagger \Sigma H, \\ V_Q &= y_u \bar{Q}_L \tilde{H} u_R + y_d \bar{Q}_L H d_R + \text{h.c.},\end{aligned}\tag{6}$$

where  $\langle \dots \rangle$  denotes the trace,  $Y_i s, i = 1, 2, 3$  are dimensional parameters while  $Z_i s, i = 1, 2, 3$  are dimensionless.  $H$  is the SM Higgs doublet,  $\Sigma$  is the real triplet.  $\tilde{H} = i\sigma_2 H^*$ .  $y_u$  and  $y_d$  are diagonal Yukawa coupling matrices in flavor space for simplicity. Due to the gauge structure, there are no interactions between fermion fields and the triplet.

After spontaneously symmetry breaking (SSB), we can write the doublet and triplet in a non-linear representation as [74]

$$H = U \begin{pmatrix} \chi^+ \\ \frac{1}{\sqrt{2}}(v_H + h^0 + i\chi^0) \end{pmatrix}, \quad U \equiv \exp \left( \frac{i\pi_i \sigma_i}{v_{\text{EW}}} \right) \tag{7}$$

$$\Sigma = U \Phi U^\dagger, \quad \Phi = \phi_i \sigma_i / 2 = \frac{1}{2} \begin{pmatrix} v_\Sigma + \phi^0 & \phi_1 - i\phi_2 \\ \phi_1 + i\phi_2 & -v_\Sigma - \phi^0 \end{pmatrix}, \tag{8}$$

with

$$\chi^\pm = 2 \frac{v_H}{v_\Sigma} \phi^\pm, \quad \chi^0 = 0, \tag{9}$$

where  $\sigma_i, i = 1, 2, 3$  are Pauli matrices,  $v_H$  and  $v_\Sigma$  are vacuum expectation values (VEV) of the doublet and the triplet,  $h^0$  and  $\phi^0$  are the radial modes associated to the VEV directions, and the unitary matrix  $U$  encapsulate three Goldstones  $\pi_i$ s,  $v_{\text{EW}} \equiv \sqrt{v_H^2 + 4v_\Sigma^2} \simeq 246 \text{ GeV}$  are the electroweak VEV,  $\phi^\pm = \frac{1}{\sqrt{2}}(\phi_1 \mp i\phi_2)$  is a pair of charged Higgs bosons,  $\phi^0 = -v_\Sigma + \phi_3$ . In this non-linear representation the physical states are factored out from the Goldstone matrix  $U$ , so that “integrating out” the heavy states is straightforward.

## 2. Linear Relations Between Squared Masses and UV Lagrangian Parameters

After minimizing the potential in Eq. (6), we have the following relations

$$Y_1^2 = -Z_1 v_H^2 - \frac{Z_3 v_\Sigma^2}{2} + Y_3 v_\Sigma, \quad Y_2^2 = -Z_2 v_\Sigma^2 - \frac{Z_3 v_H^2}{2} + \frac{Y_3 v_H^2}{2 v_\Sigma}, \quad (10)$$

which allows us to express the couplings  $Y_{1,2}$  in terms of the vacuum expectation values  $v_{H,\Sigma}$ .

With nonzero values of  $v_H$  and  $v_\Sigma$ , the mass terms after symmetry breaking are given by

$$\mathcal{L}_{\text{mass}} = \frac{1}{2} \begin{pmatrix} h^0 & \phi^0 \end{pmatrix} \begin{pmatrix} 2Z_1 v_H^2 & v_H (Z_3 v_\Sigma - Y_3) \\ v_H (Z_3 v_\Sigma - Y_3) & 2Z_2 v_\Sigma^2 + \frac{Y_3 v_H^2}{2 v_\Sigma} \end{pmatrix} \begin{pmatrix} h^0 \\ \phi^0 \end{pmatrix} + (v_H^2 + 4v_\Sigma^2)^2 \frac{Y_3}{2v_\Sigma v_H^2} \phi^+ \phi^- \quad (11)$$

where  $h^0$  and  $\phi^0$  are neutral Higgs bosons and  $\phi^\pm$  are charged Higgs bosons. The neutral fields  $h^0$  and  $\phi^0$  can then be rotated into the mass eigenstates  $h$  and  $K$  via a mixing angle  $\gamma$ <sup>5</sup>,

$$\begin{pmatrix} h \\ K \end{pmatrix} = \begin{pmatrix} c_\gamma & -s_\gamma \\ s_\gamma & c_\gamma \end{pmatrix} \begin{pmatrix} h^0 \\ \phi^0 \end{pmatrix}, \quad \tan(2\gamma) = \frac{v_H (Z_3 v_\Sigma - Y_3)}{Z_2 v_\Sigma^2 - Z_1 v_H^2 + \frac{Y_3 v_H^2}{4 v_\Sigma}}, \quad (12)$$

where  $h$  represents the discovered 125 GeV Higgs, and  $K$  represents a heavy neutral scalar.

The masses of  $h$  and  $K$  are given by

$$m_{h,K}^2 = Z_1 v_H^2 + Z_2 v_\Sigma^2 + \frac{Y_3 v_H^2}{4 v_\Sigma} \mp \sqrt{\left( Z_1 v_H^2 - Z_2 v_\Sigma^2 - \frac{Y_3 v_H^2}{4 v_\Sigma} \right)^2 + v_H^2 (Z_3 v_\Sigma - Y_3)^2}. \quad (13)$$

Meanwhile, the mass of the charged Higgs bosons is given by

$$m_{\phi^\pm}^2 = (v_H^2 + 4v_\Sigma^2) \frac{Y_3}{2 v_\Sigma} = v_{\text{EW}}^2 \frac{Y_3}{2 v_\Sigma}. \quad (14)$$

It is useful to rewrite the Lagrangian parameters in terms of physical masses, mixing angles, and VEVs. Apart from  $Y_1$  and  $Y_2$ , the other four parameters are given by

$$\begin{aligned} Y_3 &= \frac{2v_\Sigma}{v_H^2 + 4v_\Sigma^2} m_{\phi^\pm}^2 \\ Z_1 &= \frac{1}{2v_H^2} (c_\gamma^2 m_h^2 + s_\gamma^2 m_K^2) \\ Z_2 &= \frac{1}{2v_\Sigma^2} \left( s_\gamma^2 m_h^2 + c_\gamma^2 m_K^2 - \frac{v_H^2}{v_H^2 + 4v_\Sigma^2} m_{\phi^\pm}^2 \right) \\ Z_3 &= \frac{1}{v_H v_\Sigma} \left[ s_\gamma c_\gamma (m_K^2 - m_h^2) + \frac{2v_H v_\Sigma}{v_H^2 + 4v_\Sigma^2} m_{\phi^\pm}^2 \right]. \end{aligned} \quad (15)$$

---

<sup>5</sup> Throughout this work, we use the shorthand notation  $s_x \equiv \sin(x)$ ,  $c_x \equiv \cos(x)$  for any angle  $x$ .

From these expressions, we see that the four parameters are linearly proportional to the squares of the scalar masses, such as  $m_h^2$ ,  $m_K^2$  and  $m_{\phi^\pm}^2$ . Moreover, combining these results with Eq. (10),  $Y_1^2$  and  $Y_2^2$  are also linearly proportional to the squared masses. This behavior arises because the physical masses of neutral states are the eigenvalues of the mass matrix (see Eq. (11)), which depends linearly on the Lagrangian parameters and is diagonalized by an orthogonal rotation matrix characterized by the mixing angle  $\gamma$ , while the physical mass of charged states is also linearly proportional to a Lagrangian parameter. Parameterized by the VEVs and the mixing angle  $\gamma$ , this linear correspondence is a generic feature of Standard Model extensions with additional scalars [72, 80, 81].

### III. HEFTS OF THE RHTM

The tree-level matching procedure follows the methodology established in Refs. [72, 74, 80, 82–84], wherein heavy states are integrated out via the functional method. Specifically, starting from the UV Lagrangian, we adopt a systematic power-counting scheme and integrate out the heavy degrees of freedom by solving their classical EoMs. The resulting operators are subsequently projected onto a complete basis [32]. Throughout this procedure, there is considerable freedom in selecting both the initial parameter set and the corresponding power-counting scheme. These choices result in several distinct HEFT formulations [72]. To clarify their interrelations, we first examine HEFTs derived from a common parameter set under different power-counting rules. Subsequently, we investigate the variations arising from different parameter sets, each associated with its own respective power-counting scheme.

#### A. Primary HEFT and decoupling HEFT

##### 1. Parameter Set

In Ref. [84], we adopted the parameter set  $\{Z_1, Z_2, Z_3, Y_3, v_H, \xi\}$  and defined the power counting via an expansion in  $\xi \equiv v_\Sigma/v_H$ . This framework describes a decoupling limit: as the heavy degrees of freedom are integrated out, the theory reduces to the SM at the lowest order of the expansion. However, this choice is not optimal for revealing possible non-decoupling effects. To address this point, it is advantageous to adopt a parameter set in which the

heavy scalar masses and the mixing angle  $s_\gamma$  (see Eq. (12)) are explicit. Unlike the previous set, where these quantities were implicit, this choice directly exposes non-decoupling effects; in particular,  $s_\gamma$  can remain finite even after the heavy states are integrated out, signaling a departure from the standard decoupling limit. Accordingly, we choose the following set of independent parameters for our analysis:

$$\{m_{\phi^\pm}, m_K, m_h, s_\gamma, v_{\text{EW}}, \xi\}, \quad (16)$$

where  $m_{\phi^\pm}$  and  $m_K$  represent the masses of the heavy charged and neutral scalars, respectively.

## 2. Power Countings

In the UV–SMEFT matching procedure [62, 63, 84], the power counting is performed by expanding in the ratio  $(v_{\text{EW}}/Y_2)^2$ , where  $Y_2$  denotes the mass parameter of the real triplet. Upon electroweak symmetry breaking, the mass degeneracy within the triplet is lifted, resulting in two distinct physical mass eigenstates: the charged Higgs with mass  $m_{\phi^\pm}$  and the heavy neutral Higgs with mass  $m_K$ . Unlike the SMEFT approach, the UV–HEFT matching is performed by integrating out these physical fields  $\phi^\pm$  and  $K$ . Given their large masses, it is therefore natural to adopt their inverse mass squares,  $(1/m_{\phi^\pm}^2$  and  $1/m_K^2)$ , as the expansion parameters. This leads to a two-parameter expansion.

When multiple expansion parameters are involved, their relative importance must be regulated by specifying their scaling behaviors within a consistent power-counting scheme. Following the approach in Refs. [83, 85], we introduce an auxiliary parameter  $t$  to track these weights,

$$m_{\phi^\pm}^2 \sim m_K^2 \sim \mathcal{O}(t^{-1}), \quad m_h \sim v_{\text{EW}} \sim s_\gamma \sim \xi \sim \mathcal{O}(t^0), \quad (17)$$

where the large masses of the heavy fields serve as expansion parameters, while parameters such as the mixing angle  $s_\gamma$  and the VEV ratio  $\xi$  remain unsuppressed, capturing the non-decoupling effects characteristic of the HEFT framework. Moreover, as a result of the linear relations between the Lagrangian parameters and the heavy mass squares (see Eq. (15)), except for the propagator, there is no additional inverse-mass expansion when integrating out the heavy states, this scheme preserves the maximal amount of UV information. Consequently, we refer to the resulting effective theory as the primary HEFT (pHEFT).

Another possible scaling is:

$$m_{\phi^\pm}^2 \sim m_K^2 \sim \mathcal{O}(t^{-1}), \quad m_h \sim v_{\text{EW}} \sim \mathcal{O}(t^0), \quad s_\gamma \sim \xi \sim \mathcal{O}(t^1), \quad (18)$$

where the mixing angle  $s_\gamma$  and the VEV ratio  $\xi$  are suppressed by the heavy scales. In the limit  $m_{\phi^\pm, K}^2 \rightarrow \infty$  (i.e.,  $t \rightarrow 0$ ), these parameters vanish, thereby satisfying the requirements for a decoupling scenario. We refer to the theory under this power-counting as the decoupling HEFT (dHEFT).

### 3. The matching results

Using the parameter set in Eq. (16) the Lagrangian is written as

$$\begin{aligned} \mathcal{L} \supset \mathcal{L}_{\text{kin}}(v_{\text{EW}}, \xi; \phi_1, \phi_2, K, h, U) - V_S(m_{\phi^\pm}^2, m_K^2, m_h, v_{\text{EW}}, s_\gamma, \xi; \phi_1, \phi_2, K, h, U) \\ - V_Q(y_u, y_d; \phi_1, \phi_2, K, h, U), \end{aligned} \quad (19)$$

where  $\phi_1, \phi_2, K$  are heavy Higgses that will be integrated out. We use two real fields  $\phi_{1,2}$  instead of  $\phi^\pm$  in calculation for simplicity. Their EoMs are

$$\partial_\mu \left[ \frac{\partial \mathcal{L}}{\partial (\partial_\mu H^a)} \right] - \frac{\partial \mathcal{L}}{\partial H^a} = 0, \quad H^a = (K, \phi_1, \phi_2). \quad (20)$$

We solve the EoMs through a  $t$ -dependent series expansion. The heavy states are expanded as

$$\begin{aligned} K &= K_0 + K_1 + K_2 + \dots, \\ \phi_1 &= \phi_{10} + \phi_{11} + \phi_{12} + \dots, \\ \phi_2 &= \phi_{20} + \phi_{21} + \phi_{22} + \dots, \end{aligned} \quad (21)$$

where  $K_0 \sim \mathcal{O}(t^0)$ ,  $K_1 \sim \mathcal{O}(t^1)$ ,  $K_2 \sim \mathcal{O}(t^2)$ , and so on. Similar scaling behavior is assumed for  $\phi_{1i}$  and  $\phi_{2i}$ . As the explicit solutions for  $K_i$  and  $\phi_{1i,2i}$  are lengthy, we present them in Appendix A. Substituting the solutions for the heavy fields into the original Lagrangian, we obtain the effective HEFT Lagrangian. In the following, we directly present the results for the pHEFT and dHEFT and analyze their relations.

With the definition  $V_\mu \equiv U^\dagger D_\mu U$ , the Lagrangian of the primary HEFT up to  $\mathcal{O}(t^0)$  takes

the form:

$$\begin{aligned} \mathcal{L}_{\text{HEFT}}^p(t^{-1}) &= \frac{v_H^2 [(4\xi^2 + 1)m_K^2(s_\gamma + \xi c_\gamma)^2 - \xi^2 m_{\phi^\pm}^2]}{8(4\xi^2 + 1)} - \frac{h^3 m_{\phi^\pm}^2 s_\gamma^2 (2\xi c_\gamma + s_\gamma)}{2\xi(4\xi^2 + 1)v_H} \\ &\quad - \frac{h^4}{8\xi^2(4\xi^2 + 1)^2 v_H^2 m_K^2} \left\{ m_{\phi^\pm}^2 s_\gamma^2 \left[ (4\xi^2 + 1)m_K^2 \left( 6(2\xi^2 - 1)c_\gamma^4 + 7c_\gamma^2 + 18\xi c_\gamma^3 s_\gamma - 4\xi c_\gamma s_\gamma - 1 \right) \right. \right. \\ &\quad \left. \left. + m_{\phi^\pm}^2 \left( 9(1 - 4\xi^2)c_\gamma^4 + 3(8\xi^2 - 3)c_\gamma^2 - 36\xi c_\gamma^3 s_\gamma + 12\xi c_\gamma s_\gamma - 4\xi^2 \right) \right] \right\} + \mathcal{O}(h^5), \end{aligned} \quad (22)$$

$$\begin{aligned} \mathcal{L}_{\text{HEFT}}^p(t^0) &= \frac{1}{2} \langle V_\mu \sigma_3 \rangle \langle V^\mu \sigma_3 \rangle \left\{ \xi^2 v_H^2 - 2h\xi v_H s_\gamma + h^2 s_\gamma \left[ s_\gamma^3 - \xi c_\gamma^3 + \frac{c_\gamma m_{\phi^\pm}^2 (3c_\gamma s_\gamma + 4\xi - 6\xi s_\gamma^2)}{(4\xi^2 + 1)m_K^2} \right] + \mathcal{O}(h^3) \right\} \\ &\quad + \frac{1}{4} \langle V_\mu V^\mu \rangle \left\{ -(4\xi^2 + 1)v_H^2 - 2hv_H(c_\gamma - 4\xi s_\gamma) + \frac{h^2}{\xi} \left[ c_\gamma s_\gamma (4\xi^2 c_\gamma^2 + s_\gamma^2) \right. \right. \\ &\quad \left. \left. + \xi(-5s_\gamma^4 + 2s_\gamma^2 - 1) + \frac{m_{\phi^\pm}^2 s_\gamma (3(8\xi^2 - 1)c_\gamma s_\gamma^2 - 16\xi^2 c_\gamma + 2\xi(9s_\gamma^2 - 8)s_\gamma)}{(4\xi^2 + 1)m_K^2} \right] + \mathcal{O}(h^3) \right\} \\ &\quad + \frac{1}{2} D_\mu h D^\mu h + \frac{1}{8} m_h^2 v_H^2 (c_\gamma - \xi s_\gamma)^2 - \frac{1}{2} h^2 m_h^2 + \frac{h^3 m_h^2 (s_\gamma^3 - \xi c_\gamma^3)}{2\xi v_H} \\ &\quad + \frac{h^4 m_h^2}{24\xi^2(4\xi^2 + 1)^2 v_H^2 m_K^4} \left\{ 4m_{\phi^\pm}^4 s_\gamma^2 (3c_\gamma s_\gamma + 4\xi - 6\xi s_\gamma^2)^2 \right. \\ &\quad \left. + (4\xi^2 + 1)^2 m_K^4 \left[ s_\gamma^2 (38\xi c_\gamma^3 s_\gamma + 25\xi^2 + 19(\xi^2 - 1)s_\gamma^4 + (16 - 41\xi^2)s_\gamma^2) - 3\xi^2 \right] \right. \\ &\quad \left. - 20(4\xi^2 + 1)m_K^2 m_{\phi^\pm}^2 s_\gamma^2 \left[ \xi c_\gamma s_\gamma (7 - 9s_\gamma^2) - c_\gamma^2 ((6\xi^2 - 3)s_\gamma^2 - 4\xi^2) \right] \right\} + \mathcal{O}(h^5) \\ &\quad + \bar{Q}_L U \begin{pmatrix} y_u & 0 \\ 0 & y_d \end{pmatrix} Q_R \times \frac{1}{\sqrt{2}} \left\{ -v_H - hc_\gamma \right. \\ &\quad \left. + \frac{h^2 s_\gamma^2 [(4\xi^2 + 1)c_\gamma m_K^2 (\xi c_\gamma + s_\gamma) - m_{\phi^\pm}^2 (3c_\gamma s_\gamma + 4\xi - 6\xi s_\gamma^2)]}{2\xi(4\xi^2 + 1)v_H m_K^2} + \mathcal{O}(h^3) \right\} + \text{h.c.}, \end{aligned} \quad (23)$$

where  $v_H \equiv v_{\text{EW}}/\sqrt{1 + 4\xi^2}$  is used to avoid overly lengthy expressions, the covariant derivative  $D_\mu$  acting on the Higgs boson  $h$  reduces to the ordinary partial derivative,  $\partial_\mu$ , since it is a gauge singlet, and the kinetic term for the Higgs field  $h$  has already been brought into its canonical form via a field redefinition. The primary HEFT starts at  $\mathcal{O}(t^{-1})$ , with terms proportional to  $m_K^2$ ,  $m_{\phi^\pm}^2$ , or their combinations. At the order  $\mathcal{O}(t^0)$ , in addition to the terms present in the Standard Model,

$$\begin{aligned} \mathcal{L}_{\text{SM}} &= \frac{1}{2} D_\mu h D^\mu h - \frac{1}{4} (v_{\text{EW}} + h)^2 \langle V_\mu V^\mu \rangle + \frac{m_h^2 (v_{\text{EW}} + h)^2 (v_{\text{EW}}^2 - 2hv_{\text{EW}} - h^2)}{8v_{\text{EW}}^2} \\ &\quad - \frac{v_{\text{EW}} + h}{\sqrt{2}} \bar{Q}_L U \begin{pmatrix} y_u & 0 \\ 0 & y_d \end{pmatrix} Q_R + \text{h.c.}, \end{aligned} \quad (24)$$

the remaining terms proportional to  $s_\gamma$ ,  $c_\gamma$ , and  $\xi$  encode the non-decoupling effects of the heavy fields.

The decoupling HEFT Lagrangian to the first few orders in the power counting is given by

$$\begin{aligned} \mathcal{L}_{\text{HEFT}}^d(t^0) &= \frac{1}{2} D_\mu h D^\mu h - \frac{1}{4} (v_{\text{EW}} + h)^2 \langle V_\mu V^\mu \rangle + \frac{m_h^2 (v_{\text{EW}} + h)^2 (v_{\text{EW}}^2 - 2h v_{\text{EW}} - h^2)}{8v_{\text{EW}}^2} \\ &\quad - \frac{v_{\text{EW}} + h}{\sqrt{2}} \bar{Q}_L U \begin{pmatrix} y_u & 0 \\ 0 & y_d \end{pmatrix} Q_R + \text{h.c.}, \end{aligned} \quad (25)$$

$$\begin{aligned} \mathcal{L}_{\text{HEFT}}^d(t^1) &= \frac{1}{8} v_{\text{EW}}^2 \left[ m_K^2 (\xi + s_\gamma)^2 - \xi^2 m_{\phi^\pm}^2 \right] - \frac{h^3 m_{\phi^\pm}^2 s_\gamma^2 (2\xi + s_\gamma)}{2\xi v_{\text{EW}}} \\ &\quad + \frac{h^4 m_{\phi^\pm}^2 s_\gamma^2 \left[ m_{\phi^\pm}^2 (4\xi + 3s_\gamma)^2 - m_K^2 (12\xi^2 + 14\xi s_\gamma + 5s_\gamma^2) \right]}{8\xi^2 v_{\text{EW}}^2 m_K^2} + \mathcal{O}(h^5), \end{aligned} \quad (26)$$

$$\begin{aligned} \mathcal{L}_{\text{HEFT}}^d(t^2) &= \frac{1}{2} \langle V_\mu \sigma_3 \rangle \langle V^\mu \sigma_3 \rangle \left\{ \xi^2 v_{\text{EW}}^2 - 2h\xi v_{\text{EW}} s_\gamma + \frac{h^2 s_\gamma \left[ m_{\phi^\pm}^2 (4\xi + 3s_\gamma) - \xi m_K^2 \right]}{m_K^2} + \mathcal{O}(h^3) \right\} \\ &\quad + \frac{1}{4} \langle V_\mu V^\mu \rangle \left\{ h v_{\text{EW}} (4\xi^2 + 8\xi s_\gamma + s_\gamma^2) \right. \\ &\quad \left. + \frac{h^2 s_\gamma \left[ m_K^2 (4\xi^2 + 2\xi s_\gamma + s_\gamma^2) - m_{\phi^\pm}^2 (4\xi + s_\gamma)(4\xi + 3s_\gamma) \right]}{\xi m_K^2} + \mathcal{O}(h^3) \right\} \\ &\quad - \frac{1}{8} v_{\text{EW}}^2 m_h^2 (4\xi^2 + 2\xi s_\gamma + s_\gamma^2) + \frac{h^3 m_h^2 (-4\xi^3 + 3\xi s_\gamma^2 + 2s_\gamma^3)}{4\xi v_{\text{EW}}} \\ &\quad + \frac{h^4 m_h^2}{24\xi^2 v_{\text{EW}}^2 m_K^4} \left[ m_K^4 (-12\xi^4 + 25\xi^2 s_\gamma^2 + 38\xi s_\gamma^3 + 16s_\gamma^4) \right. \\ &\quad \left. - 20m_K^2 m_{\phi^\pm}^2 s_\gamma^2 (\xi + s_\gamma)(4\xi + 3s_\gamma) + 4m_{\phi^\pm}^4 s_\gamma^2 (4\xi + 3s_\gamma)^2 \right] + \mathcal{O}(h^5) \\ &\quad + \bar{Q}_L U \begin{pmatrix} y_u & 0 \\ 0 & y_d \end{pmatrix} Q_R \times \sqrt{2} \left\{ \xi^2 v_{\text{EW}} + \frac{h s_\gamma^2}{4} \right. \\ &\quad \left. + \frac{h^2 s_\gamma^2 \left[ m_K^2 (\xi + s_\gamma) - m_{\phi^\pm}^2 (4\xi + 3s_\gamma) \right]}{4\xi v_{\text{EW}} m_K^2} + \mathcal{O}(h^3) \right\} + \text{h.c.}, \end{aligned} \quad (27)$$

where  $\mathcal{L}_{\text{HEFT}}^d(t^0)$  coincides exactly with the SM Lagrangian given in Eq. (24). That is, in the limit  $t \rightarrow 0$ , the dHEFT reduces to the SM. Physically, this corresponds to taking the masses of the heavy states to infinity, in which case the dHEFT reproduces the SM, thereby manifesting its decoupling behavior. Custodial-symmetry violation first enters at  $\mathcal{O}(t^2)$  through the term  $\langle V_\mu \sigma_3 \rangle \langle V^\mu \sigma_3 \rangle$  in  $\mathcal{L}_{\text{HEFT}}^d(t^2)$ .

#### 4. The mapping from pHEFT to dHEFT

Starting from the pHEFT results in Eqs. (22)–(23), we can re-derive an EFT Lagrangian by promoting  $s_\gamma$  and  $\xi$  to  $\mathcal{O}(t)$ . Once the terms are rearranged following the revised power-counting, the results match the dHEFT expressions in Eqs. (25)–(27) exactly. Specifically, since  $s_\gamma$  and  $\xi$  are  $\mathcal{O}(t)$  in the dHEFT power-counting, the factors  $c_\gamma = \sqrt{1 - s_\gamma^2}$  and  $(1 + 4\xi^2)^{-1}$  must be Taylor-expanded as:

$$c_\gamma = 1 - \frac{s_\gamma^2}{2} - \frac{s_\gamma^4}{8} + \dots, \quad (28)$$

$$\frac{1}{1 + 4\xi^2} = 1 - 4\xi^2 + 16\xi^4 + \dots, \quad (29)$$

which only yield even powers of  $s_\gamma$  and  $\xi$ . Meanwhile, in the terms in  $\mathcal{L}_{\text{HEFT}}^{\text{p}}(t^{-1})$  and the shifted Lagrangian  $\Delta\mathcal{L}_{\text{HEFT}}^{\text{p}}(t^0) \equiv \mathcal{L}_{\text{HEFT}}^{\text{p}}(t^0) - \mathcal{L}^{\text{SM}}$ , the total power of  $s_\gamma$  and  $\xi$  is restricted to even integers starting from two.

Consequently, we obtain the following mapping:

$$\mathcal{L}_{\text{HEFT}}^{\text{p}}(t^{-1}) \rightarrow \mathcal{L}_{\text{HEFT}}^{\text{d}}(t^1) + \mathcal{S}_1 \mathcal{L}_{\text{HEFT}}^{\text{d}}(t^3) + \dots, \quad (30)$$

$$\Delta\mathcal{L}_{\text{HEFT}}^{\text{p}}(t^0) \rightarrow \mathcal{L}_{\text{HEFT}}^{\text{d}}(t^2) + \mathcal{S}_1 \mathcal{L}_{\text{HEFT}}^{\text{d}}(t^4) + \dots, \quad (31)$$

where  $\mathcal{S}_i \mathcal{L}_{\text{HEFT}}^{\text{d}}(t^n)$  denotes a distinct term of the dHEFT Lagrangian at order  $\mathcal{O}(t^n)$ . Here, the index  $i$  serves merely as a label to distinguish different disjoint subsets and does not imply any particular sequence. Notably, the power  $t^n$  within each HEFT is governed by its own power-counting rule.

A concrete example is provided by the  $\langle V_\mu \sigma_3 \rangle \langle V^\mu \sigma_3 \rangle h^2$  operator. In pHEFT, its coefficient at  $\mathcal{O}(t^0)$  is:

$$\frac{s_\gamma}{2} \left[ s_\gamma^3 - \xi c_\gamma^3 + \frac{c_\gamma m_{\phi^\pm}^2 (3c_\gamma s_\gamma + 4\xi - 6\xi s_\gamma^2)}{(4\xi^2 + 1)m_K^2} \right]. \quad (32)$$

By substituting  $c_\gamma = \sqrt{1 - s_\gamma^2}$  and applying the dHEFT scaling from Eq. (18), the factors  $c_\gamma$  and  $(1 + 4\xi^2)^{-1}$  are expanded according to Eqs. (28) and (29). The leading-order result becomes

$$\frac{s_\gamma}{2m_K^2} [m_{\phi^\pm}^2 (4\xi + 3s_\gamma) - \xi m_K^2], \quad (33)$$

which is exactly the  $\mathcal{O}(t^2)$  term in dHEFT. Any remaining terms from the expansion of Eq. (32) consist of higher powers of  $s_\gamma$  and  $\xi$ , contributing to the dHEFT Lagrangian starting from  $\mathcal{O}(t^4)$ .

The mapping at the next order follows a slightly different structure:

$$\mathcal{L}_{\text{HEFT}}^{\text{p}}(t^1) \rightarrow \mathcal{S}_2 \mathcal{L}_{\text{HEFT}}^{\text{d}}(t^3) + \mathcal{S}_2 \mathcal{L}_{\text{HEFT}}^{\text{d}}(t^5) + \dots, \quad (34)$$

where  $\mathcal{S}_2 \mathcal{L}_{\text{HEFT}}^{\text{d}}(t^3)$  denotes the second disjoint subset of the dHEFT Lagrangian at  $\mathcal{O}(t^3)$ . This partitioning accounts for the fact  $\mathcal{L}_{\text{HEFT}}^{\text{p}}(t^{-1})$  has already populated the first subset,  $\mathcal{S}_1 \mathcal{L}_{\text{HEFT}}^{\text{d}}(t^3)$ , as shown in Eq. (30). These subsets are mutually exclusive; notably, the derivative operators at  $\mathcal{O}(t^3)$  in dHEFT belong exclusively to  $\mathcal{S}_2$ , since  $\mathcal{L}_{\text{HEFT}}^{\text{p}}(t^{-1})$  consists solely of  $h$  polynomials and does not generate derivative structures in its mapping.

We list the  $p^2$  and  $p^4$  operators of  $\mathcal{L}_{\text{HEFT}}^{\text{p}}(t^1)$  separately in Tables I and II, providing the corresponding terms in  $\mathcal{L}_{\text{HEFT}}^{\text{d}}(t^3)$  for comparison. In the Wilson coefficients, we retain only the lowest-order  $h$ -polynomials with higher-order terms provided in a supplementary document. Given that  $\mathcal{S}_2 \mathcal{L}_{\text{HEFT}}^{\text{d}}(t^3)$  captures only the leading-order contribution of the mapping, the transformation between the second and third columns of these tables is simplified via the substitutions  $c_\gamma \rightarrow 1$  and  $(1 + 4\xi^2) \rightarrow 1$  as established in Eqs. (28) and (29). Notice that  $v_H \rightarrow v_{\text{EW}}$  as  $(1 + 4\xi^2) \rightarrow 1$ .

| Operators   | WCs ( $\mathcal{L}_{\text{HEFT}}^{\text{p}}(t^1)$ )   | WCs ( $\mathcal{L}_{\text{HEFT}}^{\text{d}}(t^3)$ )   |
|---|---|---|
| $\langle V_\mu V^\mu \rangle$                                   | $\frac{h^2 m_h^2 s_\gamma (4\xi c_\gamma + s_\gamma)}{2\xi (4\xi^2 + 1) m_K^4} [2(4\xi^2 + 1) c_\gamma m_K^2 (\xi c_\gamma + s_\gamma) - m_{\phi^\pm}^2 (3c_\gamma s_\gamma + 4\xi - 6\xi s_\gamma^2)]$ | $\frac{h^2 m_h^2 s_\gamma (4\xi + s_\gamma)}{2\xi m_K^4} [2m_K^2 (\xi + s_\gamma) - m_{\phi^\pm}^2 (4\xi + 3s_\gamma)]$ |
| $\langle V_\mu \sigma_3 \rangle \langle V^\mu \sigma_3 \rangle$ | $\frac{h^2 c_\gamma m_h^2 s_\gamma}{(4\xi^2 + 1) m_K^4} [m_{\phi^\pm}^2 (3c_\gamma s_\gamma + 4\xi - 6\xi s_\gamma^2) - 2(4\xi^2 + 1) c_\gamma m_K^2 (\xi c_\gamma + s_\gamma)]$                        | $\frac{h^2 m_h^2 s_\gamma}{m_K^4} [m_{\phi^\pm}^2 (4\xi + 3s_\gamma) - 2m_K^2 (\xi + s_\gamma)]$                        |

TABLE I.  $p^2$  operators in  $\mathcal{L}_{\text{HEFT}}^{\text{p}}(t^1)$  and their corresponding Wilson coefficients (WCs). The first column lists the operators, while the second and third columns show the WCs in pHEFT and their leading-order mapping to dHEFT at  $\mathcal{O}(t^3)$ , respectively. The transformation between these columns is simplified by  $c_\gamma \rightarrow 1$  and  $(1 + 4\xi^2) \rightarrow 1$ . For brevity, higher-order  $h$ -polynomials (e.g.,  $\mathcal{O}(h^3)$ ) are omitted and provided in the supplementary files.

The mapping established in Eqs. (31) and (34) also applies to the quark sector. In  $\mathcal{L}_{\text{HEFT}}^{\text{p}}(t^0)$ , the interaction involving quark currents is given by:

$$\mathcal{L}_{\text{HEFT}}^{\text{p}}(t^0) \supset -\frac{v_{\text{EW}}(1 + 4\xi^2)^{-1/2} + h c_\gamma}{\sqrt{2}} \bar{Q}_L U \begin{pmatrix} y_u & 0 \\ 0 & y_d \end{pmatrix} Q_R + \text{h.c.}, \quad (35)$$

| Operators   | WCs ( $\mathcal{L}_{\text{HEFT}}^{\text{p}}(t^1)$ )  | WCs ( $\mathcal{L}_{\text{HEFT}}^{\text{d}}(t^3)$ )  |
|---|--|--|
| $\langle V_\mu V^\mu \rangle \langle V_\nu V^\nu \rangle$   | $v_H^2 (4\xi c_\gamma + s_\gamma)^2 / 8m_K^2$  | $v_{\text{EW}}^2 (4\xi + s_\gamma)^2 / 8m_K^2$   |
| $\langle V_\mu \sigma_3 \rangle \langle V^\mu \sigma_3 \rangle \langle V_\nu V^\nu \rangle$                                   | $-\xi c_\gamma v_H^2 (4\xi c_\gamma + s_\gamma) / 2m_K^2$  | $-\xi v_{\text{EW}}^2 (4\xi + s_\gamma) / 2m_K^2$  |
| $\langle V_\mu \sigma_3 \rangle \langle V_\nu \sigma_3 \rangle \langle V^\mu V^\nu \rangle$                                   | $\xi^2 v_H^2 / (4\xi^2 + 1) m_{\phi^\pm}^2$  | $\xi^2 v_{\text{EW}}^2 / m_{\phi^\pm}^2$   |
| $\langle V_\mu \sigma_3 \rangle \langle V^\mu \sigma_3 \rangle \langle V_\nu \sigma_3 \rangle \langle V^\nu \sigma_3 \rangle$ | $\frac{1}{2} \xi^2 v_H^2 \left[ \frac{c_\gamma^2}{m_K^2} - \frac{1}{(4\xi^2 + 1) m_{\phi^\pm}^2} \right]$  | $\frac{\xi^2 v_{\text{EW}}^2}{2m_K^2 m_{\phi^\pm}^2} (m_{\phi^\pm}^2 - m_K^2)$                                   |
| $\langle V_\mu V_\nu \sigma_3 \rangle \langle V^\mu \sigma_3 \rangle D^\nu h$   | $4\xi v_H (\xi c_\gamma + s_\gamma) / (4\xi^2 + 1) m_{\phi^\pm}^2$   | $4\xi v_{\text{EW}} (\xi + s_\gamma) / m_{\phi^\pm}^2$   |
| $\langle V_\mu V_\nu \rangle D^\mu h D^\nu h$   | $-4(\xi c_\gamma + s_\gamma)^2 / (4\xi^2 + 1) m_{\phi^\pm}^2$  | $-4(\xi + s_\gamma)^2 / m_{\phi^\pm}^2$  |
| $\langle V_\mu \sigma_3 \rangle \langle V_\nu \sigma_3 \rangle D^\mu h D^\nu h$   | $2(\xi c_\gamma + s_\gamma)^2 / (4\xi^2 + 1) m_{\phi^\pm}^2$   | $2(\xi + s_\gamma)^2 / m_{\phi^\pm}^2$   |
| $\langle V_\mu V^\mu \rangle D_\nu h D^\nu h$   | $\frac{s_\gamma (4\xi c_\gamma + s_\gamma)}{2\xi (4\xi^2 + 1) m_K^4} [m_{\phi^\pm}^2 (3c_\gamma s_\gamma + 4\xi - 6\xi s_\gamma^2) - (4\xi^2 + 1) c_\gamma m_K^2 (\xi c_\gamma + s_\gamma)]$ | $\frac{s_\gamma (4\xi + s_\gamma)}{2\xi m_K^4} [m_{\phi^\pm}^2 (4\xi + 3s_\gamma) - m_K^2 (\xi + s_\gamma)]$     |
| $\langle V_\mu \sigma_3 \rangle \langle V^\mu \sigma_3 \rangle D_\nu h D^\nu h$   | $\frac{c_\gamma s_\gamma}{(4\xi^2 + 1) m_K^4} [(4\xi^2 + 1) c_\gamma m_K^2 (\xi c_\gamma + s_\gamma) - m_{\phi^\pm}^2 (3c_\gamma s_\gamma + 4\xi - 6\xi s_\gamma^2)]$                        | $\frac{s_\gamma}{m_K^4} [m_K^2 (\xi + s_\gamma) - m_{\phi^\pm}^2 (4\xi + 3s_\gamma)]$                            |
| $D_\mu h D^\mu h D_\nu h D^\nu h$   | $\frac{s_\gamma^2}{2\xi^2 (4\xi^2 + 1)^2 v_H^2 m_K^6} [(4\xi^2 + 1) c_\gamma m_K^2 (\xi c_\gamma + s_\gamma) - m_{\phi^\pm}^2 (3c_\gamma s_\gamma + 4\xi - 6\xi s_\gamma^2)]^2$              | $\frac{s_\gamma^2}{2\xi^2 v_{\text{EW}}^2 m_K^6} [m_K^2 (\xi + s_\gamma) - m_{\phi^\pm}^2 (4\xi + 3s_\gamma)]^2$ |

TABLE II.  $p^4$  operators in  $\mathcal{L}_{\text{HEFT}}^{\text{p}}(t^1)$  and their corresponding Wilson coefficients. Following the same structure as Table I, the second column presents the pHEFT results, which reduce to the  $\mathcal{O}(t^3)$  dHEFT terms in the third column under the approximations  $c_\gamma \rightarrow 1$  and  $(1 + 4\xi^2) \rightarrow 1$ . Higher-order  $h$ -polynomials are relegated to the supplementary files.

where higher-order polynomials in  $h$  are omitted. Following the dHEFT power counting, this expression is mapped onto:

$$\mathcal{L}_{\text{HEFT}}^{\text{d}}(t^0) \supset -\frac{v_{\text{EW}} + h}{\sqrt{2}} \bar{Q}_L U \begin{pmatrix} y_u & 0 \\ 0 & y_d \end{pmatrix} Q_R + \text{h.c.}, \quad (36)$$

$$\mathcal{L}_{\text{HEFT}}^{\text{d}}(t^2) \supset \left( \sqrt{2} \xi^2 v_{\text{EW}} + \frac{hs_\gamma^2}{2\sqrt{2}} \right) \bar{Q}_L U \begin{pmatrix} y_u & 0 \\ 0 & y_d \end{pmatrix} Q_R + \text{h.c..} \quad (37)$$

Specifically, Eq. (36) represents the Standard Model Yukawa sector, while the  $\mathcal{O}(t^2)$  term in Eq. (37) provides the leading new physics correction in the decoupling limit.

We list the operators of  $\mathcal{L}_{\text{HEFT}}^{\text{p}}(t^1)$  involving fermion currents and their Wilson coefficients in Table III. Notably, the fermionic operator structures in  $\mathcal{L}_{\text{HEFT}}^{\text{d}}(t^3)$  are identical to those in the pHEFT framework. Since  $\mathcal{L}_{\text{HEFT}}^{\text{p}}(t^{-1})$  contains no fermion currents, there are no

contribution from lower-order pHEFT terms. Consequently, the Wilson coefficients for the dHEFT at  $\mathcal{O}(t^3)$  can be directly obtained from the second column of Table III by applying the leading-order substitutions  $c_\gamma \rightarrow 1$  and  $(1 + 4\xi^2) \rightarrow 1$ .

### 5. Discussion on Framework Correspondence

The pHEFT and dHEFT Lagrangians are derived via a common functional matching approach: the heavy states  $\phi^\pm$  and  $K$  are integrated out at tree level by solving their EoMs perturbatively and substituting back, which yields a series of local HEFT operators. These two HEFTs share an identical parameter set:

$$\mathcal{P} = \{m_{\phi^\pm}^2, m_K^2, m_h, v_{\text{EW}}, s_\gamma, \xi\}, \quad (38)$$

while following different power-counting schemes:

$$\begin{aligned} \text{pHEFT: } m_{\phi^\pm}^2 &\sim m_K^2 \sim \mathcal{O}(t^{-1}), & m_h \sim v_{\text{EW}} \sim s_\gamma \sim \xi &\sim \mathcal{O}(t^0), \\ \text{dHEFT: } m_{\phi^\pm}^2 &\sim m_K^2 \sim \mathcal{O}(t^{-1}), & m_h \sim v_{\text{EW}} &\sim \mathcal{O}(t^0), & s_\gamma \sim \xi &\sim \mathcal{O}(t^1). \end{aligned}$$

A comparison of the matching results reveals that the dHEFT Lagrangian can be exactly reproduced from the pHEFT results by simply applying the dHEFT power-counting scheme to the pHEFT coefficients. Specifically, by performing the Taylor expansions of  $c_\gamma$  and  $(1 + 4\xi^2)^{-1}$  as dictated by the  $s_\gamma \sim \xi \sim \mathcal{O}(t^1)$  scaling, the pHEFT expressions map exactly onto their dHEFT counterparts. Therefore, performing the pHEFT matching is sufficient: the dHEFT limit follows directly from parameter re-scaling, making a separate functional matching procedure for the decoupling case redundant.

This means that part of the matching procedure—namely, “integrating out” the heavy states and expanding in the inverse of their masses—can be separated from the full matching procedure. The pHEFT completes this core step while retaining the maximal information from the UV model. Further scalings of  $\sin \gamma$  and  $\xi$  then act as additional restrictions. In other words, a HEFT with an arbitrary scaling of the parameter set  $\mathcal{P} = \{m_{\phi^\pm}^2, m_K^2, m_h, v_{\text{EW}}, s_\gamma, \xi\}$  can be obtained by applying such a scaling directly to the pHEFT, without the need to solve the EoM or perform operator reduction. By circumventing case-by-case procedures for solving the EoMs and performing operator reductions, this approach provides a unified and efficient framework for deriving the effective limits of the underlying UV theory across different scaling schemes.

| Operator   | WCs ( $\mathcal{L}_{\text{HEFT}}^{\text{p}}(t^1)$ )   |
|--|---|
| $(\bar{Q}_L U Q_R) \langle V_\mu V^\mu \rangle + \text{h.c.}$  | $\frac{1}{2}(y_u + y_d) \frac{v_H s_\gamma (4\xi c_\gamma + s_\gamma)}{2\sqrt{2}m_K^2}$   |
| $(\bar{Q}_L U \sigma_3 Q_R) \langle V_\mu V^\mu \rangle + \text{h.c.}$                                   | $\frac{1}{2}(y_u - y_d) \frac{v_H s_\gamma (4\xi c_\gamma + s_\gamma)}{2\sqrt{2}m_K^2}$   |
| $(\bar{Q}_L U Q_R) \langle V_\mu \sigma_3 \rangle \langle V^\mu \sigma_3 \rangle + \text{h.c.}$          | $\frac{1}{2}(y_u + y_d) \left( -\frac{\xi c_\gamma v_H s_\gamma}{\sqrt{2}m_K^2} \right)$  |
| $(\bar{Q}_L U \sigma_3 Q_R) \langle V_\mu \sigma_3 \rangle \langle V^\mu \sigma_3 \rangle + \text{h.c.}$ | $\frac{1}{2}(y_u - y_d) \left( -\frac{\xi c_\gamma v_H s_\gamma}{\sqrt{2}m_K^2} \right) - \frac{1}{2}(y_u - y_d) \frac{\sqrt{2}\xi^2 v_H}{(4\xi^2+1)m_{\phi^\pm}^2}$  |
| $(\bar{Q}_L U [V_\mu, \sigma_3] Q_R) \langle V^\mu \sigma_3 \rangle + \text{h.c.}$                       | $\frac{1}{2}(y_u + y_d) \frac{\sqrt{2}\xi^2 v_H}{(4\xi^2+1)m_{\phi^\pm}^2}$   |
| $(\bar{Q}_L U V_\mu Q_R) \langle V^\mu \sigma_3 \rangle + \text{h.c.}$                                   | $(y_u - y_d) \frac{\sqrt{2}\xi^2 v_H}{(4\xi^2+1)m_{\phi^\pm}^2}$  |
| $(\bar{Q}_L U Q_R) D_\mu h D^\mu h + \text{h.c.}$  | $\frac{1}{2}(y_u + y_d) \frac{s_\gamma^2 \left\{ m_{\phi^\pm}^2 [3s_\gamma c_\gamma + 2\xi(2-3s_\gamma^2)] - (4\xi^2+1)c_\gamma m_K^2 (\xi c_\gamma + s_\gamma) \right\}}{\sqrt{2}\xi(4\xi^2+1)v_H m_K^4}$            |
| $(\bar{Q}_L U \sigma_3 Q_R) D_\mu h D^\mu h + \text{h.c.}$   | $\frac{1}{2}(y_u - y_d) \frac{s_\gamma^2 \left\{ m_{\phi^\pm}^2 [3s_\gamma c_\gamma + 2\xi(2-3s_\gamma^2)] - (4\xi^2+1)c_\gamma m_K^2 (\xi c_\gamma + s_\gamma) \right\}}{\sqrt{2}\xi(4\xi^2+1)v_H m_K^4}$            |
| $(\bar{Q}_L U [V_\mu, \sigma_3] Q_R) D^\mu h + \text{h.c.}$  | $\frac{1}{2}(y_u - y_d) \frac{2\sqrt{2}\xi(\xi c_\gamma + s_\gamma)}{(4\xi^2+1)m_{\phi^\pm}^2}$   |
| $(\bar{Q}_L U V_\mu Q_R) D^\mu h + \text{h.c.}$  | $(y_u + y_d) \frac{2\sqrt{2}\xi(\xi c_\gamma + s_\gamma)}{(4\xi^2+1)m_{\phi^\pm}^2}$  |
| $(\bar{Q}_L U \sigma_3 Q_R) \langle V_\mu \sigma_3 \rangle D^\mu h + \text{h.c.}$                        | $-\frac{1}{2}(y_u + y_d) \frac{2\sqrt{2}\xi(\xi c_\gamma + s_\gamma)}{(4\xi^2+1)m_{\phi^\pm}^2}$  |
| $(\bar{Q}_L U Q_R) + \text{h.c.}$  | $\frac{1}{2}(y_u + y_d) \frac{h^2 m_h^2 s_\gamma^2 \left\{ 2(4\xi^2+1)c_\gamma m_K^2 (\xi c_\gamma + s_\gamma) - m_{\phi^\pm}^2 [3s_\gamma c_\gamma + 2\xi(2-3s_\gamma^2)] \right\}}{\sqrt{2}\xi(4\xi^2+1)v_H m_K^4}$ |
| $(\bar{Q}_L U \sigma_3 Q_R) + \text{h.c.}$   | $\frac{1}{2}(y_u - y_d) \frac{h^2 m_h^2 s_\gamma^2 \left\{ 2(4\xi^2+1)c_\gamma m_K^2 (\xi c_\gamma + s_\gamma) - m_{\phi^\pm}^2 [3s_\gamma c_\gamma + 2\xi(2-3s_\gamma^2)] \right\}}{\sqrt{2}\xi(4\xi^2+1)v_H m_K^4}$ |
| $(\bar{Q}_L U Q_R)(\bar{Q}_L U Q_R) + \text{h.c.}$   | $\frac{1}{4}(y_u + y_d)^2 \frac{s_\gamma^2}{4m_K^2}$  |
| $(\bar{Q}_L U Q_R)(\bar{Q}_L U \sigma_3 Q_R) + \text{h.c.}$  | $\frac{1}{2}(y_u^2 - y_d^2) \frac{s_\gamma^2}{4m_K^2}$  |
| $(\bar{Q}_L U \sigma_3 Q_R)(\bar{Q}_L U \sigma_3 Q_R) + \text{h.c.}$                                     | $\frac{1}{4}(y_u - y_d)^2 \frac{s_\gamma^2}{4m_K^2} + \frac{1}{4}y_u y_d \frac{4\xi^2}{(4\xi^2+1)m_{\phi^\pm}^2}$   |
| $(\bar{Q}_L \sigma^I U Q_R)(\bar{Q}_L \sigma^I U Q_R) + \text{h.c.}$                                     | $-\frac{1}{4}y_u y_d \frac{4\xi^2}{(4\xi^2+1)m_{\phi^\pm}^2}$   |
| $(\bar{Q}_L \gamma_\mu Q_L)(\bar{Q}_R \gamma^\mu Q_R)$   | $\frac{1}{4}(y_u^2 + y_d^2) \frac{s_\gamma^2}{4m_K^2} + \frac{1}{8}(y_u^2 + y_d^2) \frac{4\xi^2}{(4\xi^2+1)m_{\phi^\pm}^2}$   |
| $(\bar{Q}_L \gamma_\mu \sigma^I Q_L)(\bar{Q}_R \gamma^\mu U^\dagger \sigma^I U Q_R)$                     | $\frac{1}{2}y_u y_d \frac{s_\gamma^2}{4m_K^2}$  |
| $(\bar{Q}_L \gamma_\mu U \sigma_3 U^\dagger Q_L)(\bar{Q}_R \gamma^\mu Q_R)$                              | $\frac{1}{4}(y_u^2 - y_d^2) \frac{s_\gamma^2}{4m_K^2} - \frac{1}{8}(y_u^2 - y_d^2) \frac{4\xi^2}{(4\xi^2+1)m_{\phi^\pm}^2}$   |
| $(\bar{Q}_L \gamma_\mu Q_L)(\bar{Q}_R \gamma^\mu \sigma_3 Q_R)$  | $\frac{1}{4}(y_u^2 - y_d^2) \frac{s_\gamma^2}{4m_K^2} + \frac{1}{8}(y_u^2 - y_d^2) \frac{4\xi^2}{(4\xi^2+1)m_{\phi^\pm}^2}$   |
| $(\bar{Q}_L \gamma_\mu U \sigma_3 U^\dagger Q_L)(\bar{Q}_R \gamma^\mu \sigma_3 Q_R)$                     | $\frac{1}{4}(y_u - y_d)^2 \frac{s_\gamma^2}{4m_K^2} - \frac{1}{8}(y_u^2 + y_d^2) \frac{4\xi^2}{(4\xi^2+1)m_{\phi^\pm}^2}$   |

TABLE III. Fermionic operators in  $\mathcal{L}_{\text{HEFT}}^{\text{p}}(t^1)$  and their corresponding Wilson coefficients (second column). The dHEFT results at  $\mathcal{O}(t^3)$  share the same operator structures, and their coefficients can be retrieved by setting  $c_\gamma \rightarrow 1$  and  $(1+4\xi^2) \rightarrow 1$ . As in previous tables, higher-order  $h$ -polynomials are omitted and provided in the supplementary files.

The mapping relations established in Eqs. (30), (31), and (34) imply that one framework is systematically embedded within the other. Specifically, we observe the following inclusion relations:

$$\begin{aligned}\mathcal{L}_{\text{HEFT}}^{\text{p}}(t^{-1}) &\supset \mathcal{L}_{\text{HEFT}}^{\text{d}}(t^1), \\ \mathcal{L}_{\text{HEFT}}^{\text{p}}(t^{-1} + t^0) &\supset \mathcal{L}_{\text{HEFT}}^{\text{d}}(t^1 + t^2), \\ \mathcal{L}_{\text{HEFT}}^{\text{p}}(t^{-1} + t^0 + t^1) &\supset \mathcal{L}_{\text{HEFT}}^{\text{d}}(t^1 + t^2 + t^3), \dots\end{aligned}\tag{39}$$

where the ellipsis denotes that this pattern persists to all higher orders. This hierarchical structure confirms that the dHEFT is effectively contained within the pHEFT expansion. We make this correspondence visually explicit by investigating the process of Higgs self-scattering  $hh \rightarrow hh$ . For all subsequent plots, we fix the Higgs mass  $m_h$  to 125 GeV and the electroweak VEV  $v_{\text{EW}}$  to 246 GeV. While experiments also impose strong bounds— $\xi \lesssim 0.015$  from the  $\rho$  parameter [86] and  $-0.10 \lesssim s_\gamma \lesssim 0.15$  from Higgs couplings [86–88]—the parameter regions displayed in our plots are not required to satisfy them fully. Usually only slight violations are allowed unless explicitly noted. Figs. 1 and 2 demonstrate that, for typical parameter values, the  $\mathcal{O}(t^n)$  result in dHEFT closely matches the  $\mathcal{O}(t^{n-2})$  result in pHEFT—a consequence of the inherent power-counting hierarchy distinguishing the two effective theories. But in extreme regions of parameter space ( $\xi = 0.1$ , though such regions have already been ruled out by experiments, we show it for illustration), the leading-order prediction in pHEFT matches the accuracy of the second- and even third-order results in dHEFT as presented in Fig. 3. This result is expected, since a sizable non-decoupling effect in the RHTM arises from custodial-symmetry breaking and is therefore only pronounced for large values of  $\xi$ .

The existence of the straightforward inclusion relations described above is a direct consequence of the specific scaling assignments for  $s_\gamma$  and  $\xi$  in the decoupling limit. As long as these parameters are treated as  $\mathcal{O}(t^n)$  with  $n \geq 0$ , the dHEFT can be viewed as a truncation of the pHEFT. For instance, if a model required a more suppressed scaling such as  $s_\gamma \sim \mathcal{O}(t^4)$  and  $\xi \sim \mathcal{O}(t^1)$ , the inclusion relations would remain valid, as both parameters continue to provide additional suppression within the pHEFT expansion. However, for more ‘exotic’ scalings—such as  $s_\gamma \sim \mathcal{O}(t^4)$  and  $\xi \sim \mathcal{O}(t^{-1})$ —the correspondence becomes less trivial, as the enhancement from  $\xi$  could potentially compete with the suppression from  $s_\gamma$  or the heavy mass expansion. Fortunately, such unconventional power-counting schemes are rarely motivated by physical considerations. Thus, for the vast majority of phenomenologi-

cally relevant scenarios, the pHEFT serves as a robust and flexible framework for generating specific effective limits.

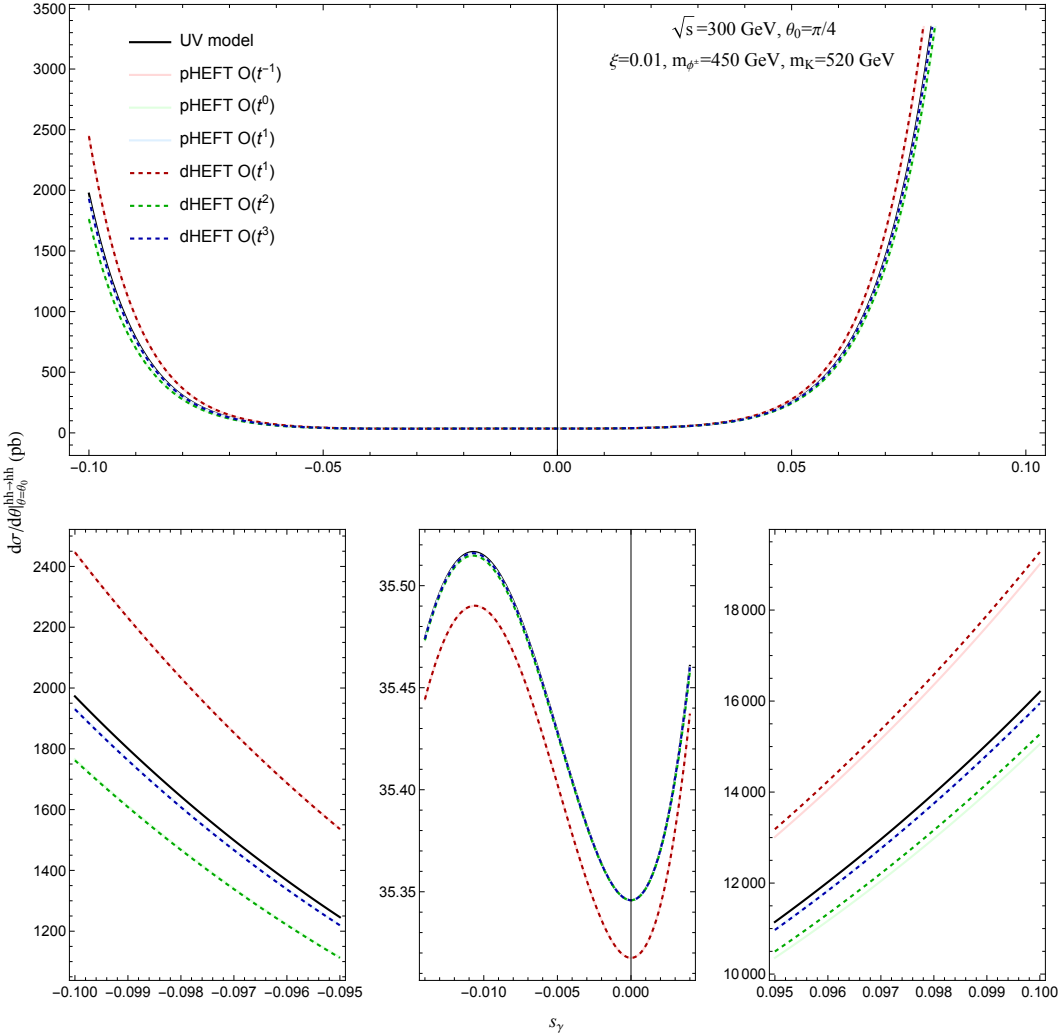


FIG. 1. Comparison between the UV model and the pHEFT and dHEFT in the differential cross-section of  $hh \rightarrow hh$ , for a center-of-mass energy  $\sqrt{s} = 300$  GeV and a scattering angle  $\theta_0 = \pi/4$ . We set  $\xi = 0.01$ ,  $m_{\phi^\pm} = 450$  GeV, and  $m_K = 520$  GeV. The Higgs mass and electroweak vacuum expectation value are fixed to their experimentally measured values:  $m_h = 125$  GeV and  $v_{EW} = 246$  GeV. The top panel presents the cross section over  $s_\gamma \in [-0.1, 0.1]$ , while the three lower panels provide detailed views of three selected subintervals.

It is also of interest to examine whether the pHEFT can provide a convenient organizational starting point for HEFT formulations based on alternative parameter sets. For instance, one may consider the set  $\{m_{\phi^\pm}^2, m_K^2, m_h, v_{EW}, Z_2, \xi\}$ , in which the physical mixing

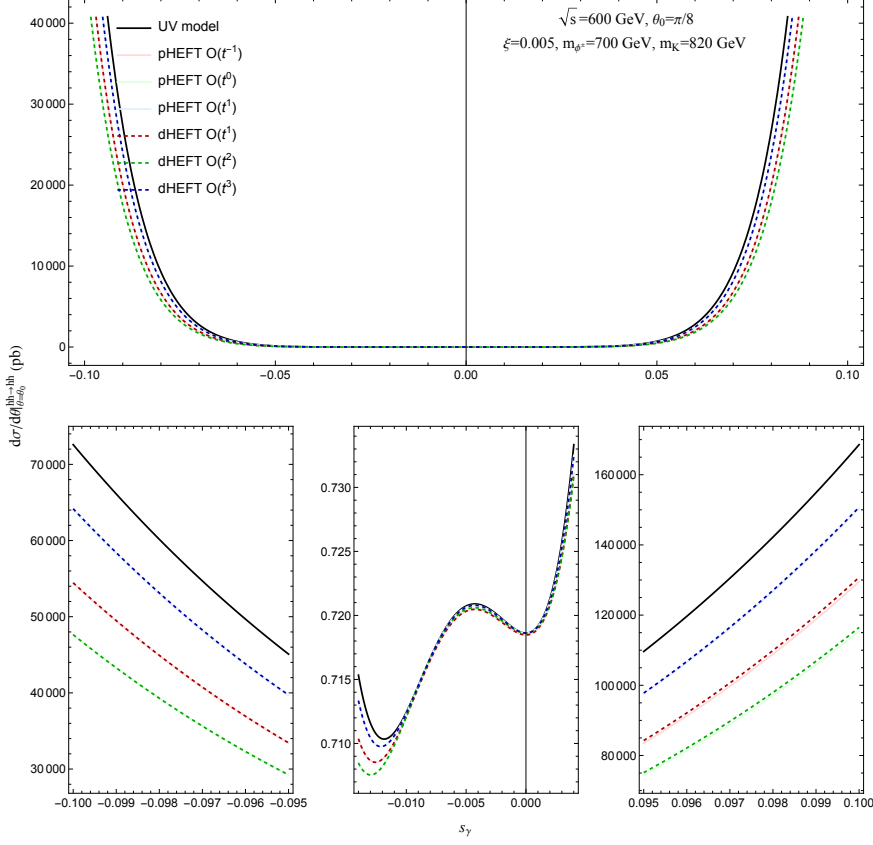


FIG. 2. Similar to Fig. 1, now shown for  $\sqrt{s} = 600$  GeV,  $\theta_0 = \pi/8$ ,  $\xi = 0.005$ ,  $m_{\phi^\pm} = 700$  GeV, and  $m_K = 820$  GeV. When  $s_\gamma > 0.084$ , the model becomes unstable because the boundedness-from-below conditions ( $Z_1, Z_2 \geq 0$  and  $|Z_3| \leq 2\sqrt{Z_1 Z_2}$  [84]) are violated.

angle  $s_\gamma$  is replaced by  $Z_2$ , a fundamental parameter appearing directly in the UV Lagrangian. Another possibility is the set  $\{Z_1, Z_2, Z_3, Y_3, v_{\text{EW}}, \xi\}$  employed in Ref. [84], where a HEFT is constructed through a systematic  $\xi$  expansion. In the following two subsections, we present a detailed analysis of these cases.

## B. $Z_2$ -HEFT

As discussed in the previous section, a Primary HEFT is obtained from UV-HEFT matching through an inverse-mass expansion without imposing additional restrictions. In principle, one may choose alternative parameter sets, including heavy-mass parameters, leading to different versions of the Primary HEFT. It is therefore important to clarify whether these formulations are equivalent and, if not, which one provides a more accurate description.

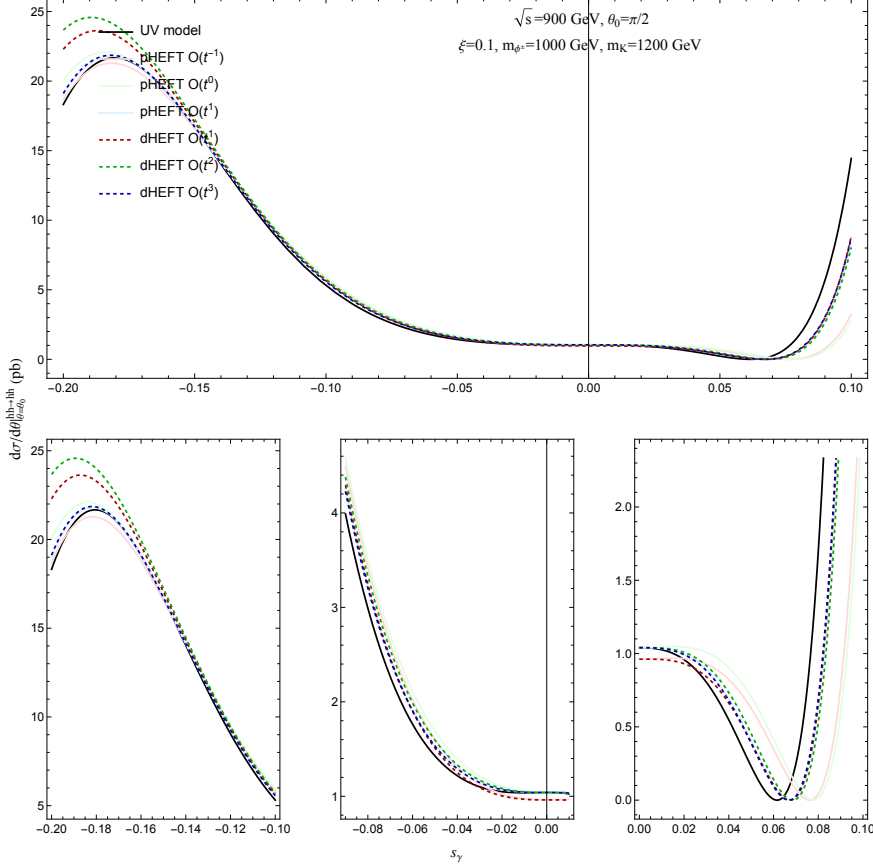


FIG. 3. Similar to Fig. 1, now shown for  $\sqrt{s} = 900$  GeV,  $\theta_0 = \pi/2$ ,  $\xi = 0.1$ ,  $m_{\phi^\pm} = 1000$  GeV, and  $m_K = 1200$  GeV. The value  $\xi = 0.1$  is chosen for illustration only and is not intended to be phenomenologically viable, having been excluded by existing measurements. When  $s_\gamma > -0.064$ , the model becomes unstable because of the boundedness-from-below conditions ( $Z_1, Z_2 \geq 0$  and  $|Z_3| \leq 2\sqrt{Z_1 Z_2}$ ) are violated.

Our baseline realization, the pHEFT, utilizes the parameter set  $\{m_{\phi^\pm}^2, m_K^2, m_h, v_{\text{EW}}, s_\gamma, \xi\}$ . Among these parameters,  $m_{\phi^\pm}^2$  and  $m_K^2$  are kept as expansion parameters; the Higgs mass  $m_h$ , the electroweak VEV  $v_{\text{EW}}$  and  $\xi$  are well-determined or constrained by precision experimental measurements. Thus,  $s_\gamma$  emerges as the most adaptable candidate for replacement. We therefore consider an alternative primary HEFT based on the set:

$$\mathcal{P}_{Z_2} = \{m_{\phi^\pm}^2, m_K^2, m_h, v_{\text{EW}}, Z_2, \xi\} \quad (40)$$

and follow a power-counting scheme:

$$Z_2\text{-HEFT: } m_{\phi^\pm}^2 \sim m_K^2 \sim \mathcal{O}(t^{-1}), \quad m_h \sim v_{\text{EW}} \sim Z_2 \sim \xi \sim \mathcal{O}(t^0). \quad (41)$$

Where the physical mixing angle  $s_\gamma$  is now treated as a derived quantity expressed in terms of the UV-Lagrangian parameter  $Z_2$  via the relation:

$$s_\gamma = \pm \sqrt{\frac{2\xi^2 Z_2 v_{\text{EW}}^2 - (4\xi^2 + 1)m_K^2 + m_{\phi^\pm}^2}{(4\xi^2 + 1)(m_h^2 - m_K^2)}}. \quad (42)$$

In this expression, the  $\pm$  sign corresponds to two distinct branches, each associated with a different HEFT. We refer to them as the positive  $Z_2$ -HEFT and the negative  $Z_2$ -HEFT, respectively.

The construction of the  $Z_2$ -HEFT then proceeds through a two-step mapping procedure. This is possible because the pHEFT already captures the full dynamics of the underlying theory, having successfully integrated out the heavy states. Consequently, the mapping requires only a parametric transformation and operator reorganization: first, we perform a substitution of  $s_\gamma$  (and  $c_\gamma$ ) into the pHEFT Lagrangian; second, we reorganize operators according to the power counting scheme in Eq. (41).

In the latter step, the expression for  $s_\gamma$  appearing on the right-hand side of Eq. (42) must be expanded in inverse powers of the heavy masses and consistently truncated at a given order. Such an expansion implicitly imposes several consistency conditions on the parameter space. For example, the appearance of the factor  $(m_h^2 - m_K^2)$  in the denominator requires the hierarchy

$$m_h^2 \ll m_K^2. \quad (43)$$

Meanwhile, regarding the numerator within the square root, a valid expansion in  $m_K^2$  and  $m_{\phi^\pm}^2$  ( $m_{\phi^\pm}^2 \sim m_K^2 \sim \mathcal{O}(t^{-1})$ ) requires the following further condition:

$$|2\xi^2 Z_2 v_{\text{EW}}^2| \ll |(4\xi^2 + 1)m_K^2 - m_{\phi^\pm}^2|. \quad (44)$$

If these two hierarchies are not maintained, the heavy-mass expansion ceases to be systematically controlled, signaling that the  $Z_2$ -HEFT no longer provides a reliable description of the RHTM.

Figs. 4 and 5 show the differential cross section for  $hh \rightarrow hh$  obtained from  $Z_2$ -HEFT, compared with that from pHEFT. For  $s_\gamma < 0$ , we use the negative  $Z_2$ -HEFT; for  $s_\gamma > 0$ , we use the positive  $Z_2$ -HEFT. The two HEFTs do not connect smoothly at  $s_\gamma = 0$ , since they approach this point from opposite directions. In Fig. 4, the  $Z_2$ -HEFT reproduces the RHTM prediction well around  $s_\gamma \simeq \pm 0.07$ . However, the accuracy decreases as  $s_\gamma$  approaches zero,

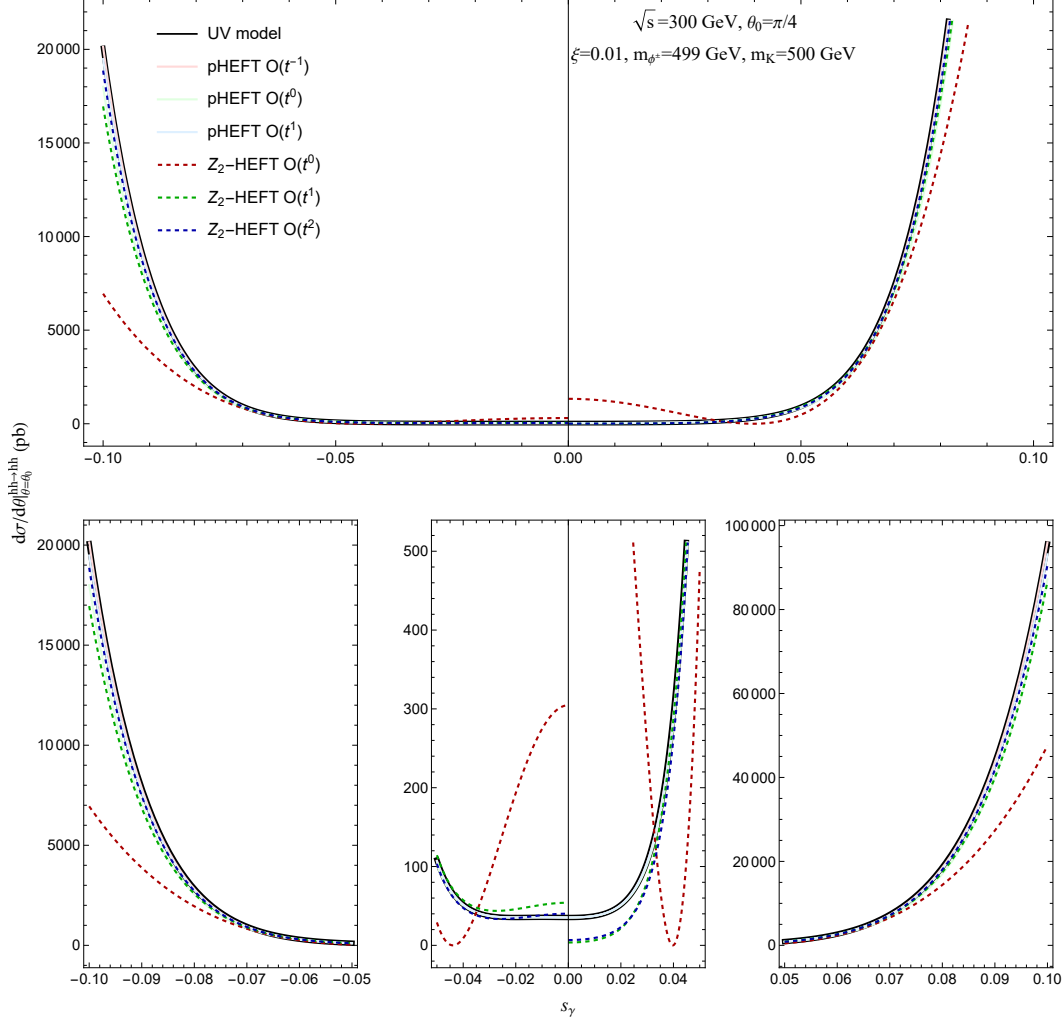


FIG. 4. Comparison between the UV model and the pHEFT and  $Z_2$ -HEFT in the differential cross-section of  $hh \rightarrow hh$ , for a center-of-mass energy  $\sqrt{s} = 300$  GeV and a scattering angle  $\theta_0 = \pi/4$ . We set  $\xi = 0.01$ ,  $m_{\phi^\pm} = 499$  GeV, and  $m_K = 500$  GeV. The Higgs mass and electroweak vacuum expectation value are fixed to their experimentally measured values:  $m_h = 125$  GeV and  $v_{EW} = 246$  GeV. The top panel presents the cross section over  $s_\gamma \in [-0.1, 0.1]$ , while the three lower panels provide detailed views of three selected subintervals.

with a more significant discrepancy observed for positive  $s_\gamma$ . This reflects the breakdown of the expansion criteria in Eq. 44 in this parameter regime. In Fig. 5, we increase the mass splitting between the charged and neutral Higgs bosons by setting  $m_{\phi^\pm} = 498$  GeV. In this case, the  $Z_2$ -HEFT exhibits good agreement with the RHTM around  $s_\gamma \simeq \pm 0.09$ . This can be understood from the fact that a larger mixing angle enhances the mass splitting between the scalar states. It is also noticeable from both Fig. 4 and Fig. 5 that the boundedness-from-

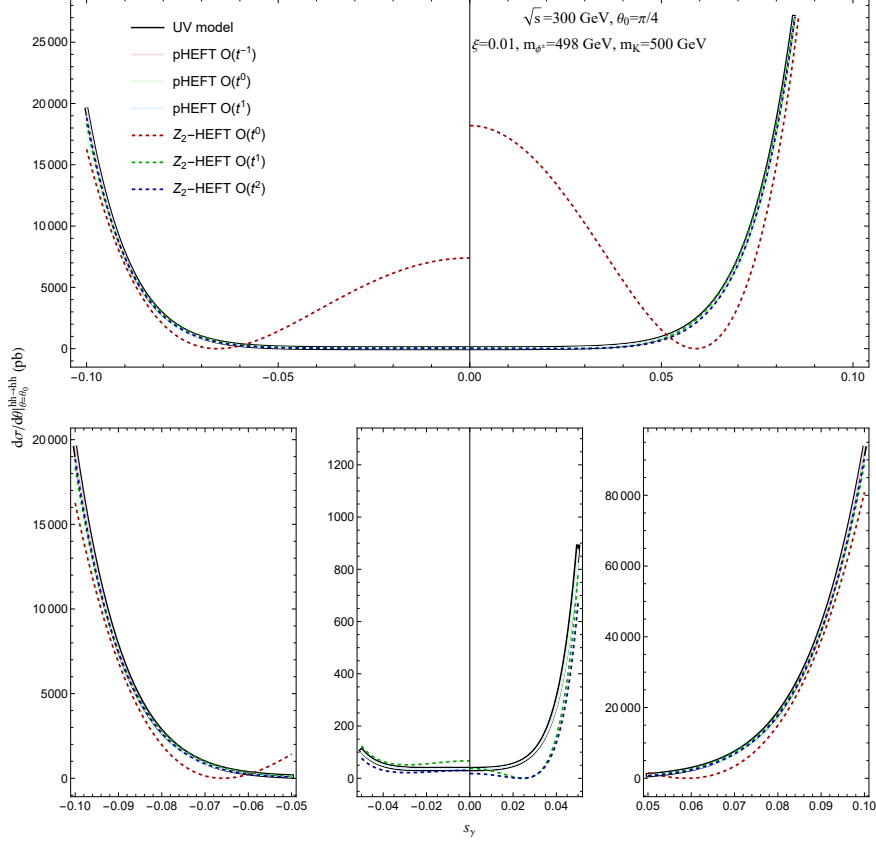


FIG. 5. Similar to Fig. 4, now shown for  $\sqrt{s} = 300$  GeV,  $\theta_0 = \pi/4$ ,  $\xi = 0.01$ ,  $m_{\phi^\pm} = 498$  GeV, and  $m_K = 500$  GeV.

below condition is almost satisfied for  $s_\gamma \in [-0.04, 0.0]$ , which is far from the region where the approximation works well. This further reinforces the conclusion that the  $Z_2$ -HEFT cannot be regarded as a viable primary HEFT.

In summary, the pHEFT framework is significantly less constrained than the  $Z_2$ -HEFT. The criteria for determining whether a parameter set retains the maximal information from the UV theory depends on whether the relation between the UV Lagrangian couplings ( $Z_i, Y_i$ ) and squared heavy masses is linear or necessitates an additional inverse-mass expansion during the matching procedure. In the RHTM, the relation between the Lagrangian couplings ( $Z_i, Y_i$ ) and the pHEFT set  $\{m_{\phi^\pm}^2, m_K^2, m_h, v_{EW}, s_\gamma, \xi\}$  is linear, as shown in Eq. (15). This linearity ensures that the UV interaction terms remain exact, avoiding the need for further expansions in inverse heavy masses. Consequently, the pHEFT parameter set preserves maximal information from the UV theory within the primary HEFT. In contrast, the  $Z_2$ -HEFT relies on non-linear relations; substituting Eq. (42) into Eq. (15) necessitates

an extra inverse-mass expansion, which introduces truncation errors and an inherent loss of precision.

It is interesting to note that in the UV models with scalar extensions, the existence of such linearity relations between the squared heavy masses and the UV Lagrangian parameters is a common feature, as seen in the  $Z_2$ -symmetric singlet model and the 2HDM in our following discussions in Sec. IV. This makes the physical basis—comprising physical masses, mixing angles, and VEVs—a naturally superior choice for defining a primary HEFT.

### C. $\xi$ -HEFT

In Ref. [84], we derived the  $\xi$ -HEFT, which utilizes the parameter set:

$$\mathcal{P}_\xi = \{Z_1, Z_2, Z_3, Y_3, v_H, \xi\} \quad (45)$$

This framework employs a  $\xi$ -expansion, which is formally equivalent to the power-counting scheme:

$$\xi\text{-HEFT: } Z_1 \sim Z_2 \sim Z_3 \sim Y_3 \sim v_H \sim \mathcal{O}(t^0), \quad \xi \sim \mathcal{O}(t^1). \quad (46)$$

In Ref. [84], the corresponding UV-to-HEFT matching results are given by

$$\begin{aligned} \mathcal{L}_{\text{HEFT}}^\xi(t^0) &= \frac{1}{2} D_\mu h D^\mu h - \frac{1}{4} Z_1 (-v_H^4 + 4h^2 v_H^2 + 4h^3 v_H + h^4) - \frac{1}{4} (v_H + h)^2 \langle V_\mu V^\mu \rangle \\ \mathcal{L}_{\text{HEFT}}^\xi(t^1) &= \frac{\xi Y_3}{4v_H} (-v_H^4 + 4h^2 v_H^2 + 4h^3 v_H + h^4) \\ \mathcal{L}_{\text{HEFT}}^\xi(t^2) &= \frac{\xi^2}{4v_H^2} \left\{ v_H^6 Z_3 + 8h^2 v_H^4 (2Z_1 - Z_3) + 8h^3 v_H^3 (5Z_1 - 2Z_3) \right. \\ &\quad + \frac{14}{3} h^4 v_H^2 (8Z_1 - 3Z_3) - 4 (v_H^4 + 3h v_H^3 + 4h^2 v_H^2) \langle V_\mu V^\mu \rangle \\ &\quad \left. + 2 (v_H^4 + 4h v_H^3 + 6h^2 v_H^2) \langle V_\mu \sigma_3 \rangle \langle V^\mu \sigma_3 \rangle \right\}, \end{aligned} \quad (47)$$

where  $h$  polynomials of higher orders have been omitted.

To facilitate a direct comparison between the pHEFT and the  $\xi$ -HEFT, first we start from the pHEFT and express its parameters  $\{m_{\phi^\pm}^2, m_K^2, m_h^2, s_\gamma, v_{\text{EW}}\}$  in terms of  $\{Z_1, Z_2, Z_3, Y_3, v_H\}$

through a systematic expansion in  $\xi$ :

$$\begin{aligned}
m_{\phi^\pm}^2 &\rightarrow \frac{Y_3 v_H}{2\xi} + 2\xi Y_3 v_H, \\
m_K^2 &\rightarrow \frac{Y_3 v_H}{2\xi} + 2\xi Y_3 v_H + 2\xi^2 v_H^2 (4Z_1 + Z_2 - 2Z_3) + O(\xi^3), \\
m_h^2 &\rightarrow 2Z_1 v_H^2 - 2\xi Y_3 v_H - 4\xi^2 v_H^2 (2Z_1 - Z_3) + O(\xi^3), \\
s_\gamma &\rightarrow -2\xi - \frac{2(4Z_1 - Z_3)\xi^2 v_H}{Y_3} + O(\xi^3), \\
v_{\text{EW}} &\rightarrow v_H + 2\xi^2 v_H + O(\xi^3).
\end{aligned} \tag{48}$$

Then we substitute these expansions into the pHEFT Lagrangian (Eq. (23)) and reorganize the resulting operators according to the  $\xi$ -HEFT power-counting scheme defined in Eq. (46). Finally, we obtain a new HEFT that is identical to the  $\xi$ -HEFT presented in Eq. (47). This demonstrates that the  $\xi$ -HEFT can be systematically derived from the pHEFT via the corresponding parameter transformation and  $\xi$ -expansion.

It is noteworthy that the leading-order scaling in  $\xi$ -HEFT (Eq. (46)) is effectively equivalent to the dHEFT scaling:  $m_{\phi^\pm}^2 \sim m_K^2 \sim \mathcal{O}(t^{-1})$ ,  $m_h \sim v_{\text{EW}} \sim \mathcal{O}(t^0)$ , and  $s_\gamma \sim \xi \sim \mathcal{O}(t^1)$ . This equivalence motivates a closer examination of the relationship between these two HEFTs. By applying the reparameterization in Eq. (48) to the dHEFT, we indeed re-derive the  $\xi$ -HEFT results presented in Eq. (47). Considering the higher-order terms discarded at each stage of the pHEFT  $\rightarrow$  dHEFT and dHEFT  $\rightarrow$   $\xi$ -HEFT mappings, the hierarchical relationship among these three HEFTs can be expressed as:

$$\text{pHEFT} \supset \text{dHEFT} \supset \xi\text{-HEFT}. \tag{49}$$

This nesting structure reveals that although pHEFT and dHEFT are formally reducible to  $\xi$ -HEFT, they encode a more fundamental matching. Specifically, the matching procedure dictates that the  $\xi$  expansion must be viewed as secondary, to be performed only after the primary inverse-mass expansion. This precedence arises from the fact that the essence of UV-EFT matching lies in the treatment of heavy-state propagators. Thus, the expansion in inverse mass is fundamental, while any expansion in additional parameters is necessarily subordinate.

The pHEFT and dHEFT frameworks improve numerical agreement with the underlying UV theory by retaining—rather than truncating—subsets of higher-order terms within their

physical parameter definitions, as seen through the inverse of Eq. (48). This approach systematically minimizes the UV–EFT mismatch at any fixed order of truncation.

In Fig. 6, we show the comparison among the pHEFT, the dHEFT and the  $\xi$ -HEFT<sup>6</sup>. First, the  $\xi$ -HEFT is far from exactly reproducing the RHTM when  $s_\gamma$  is positive (right panel). This is evident from the expansion of  $s_\gamma$  in  $\xi$  in Eq. (48), which indicates that the  $\xi$  expansion is valid only for negative  $s_\gamma$ . Second, as shown in the left panel,  $\xi$ -HEFT performs comparably to other HEFTs when  $\xi$  is close to  $-s_\gamma/2 = 0.2$ .

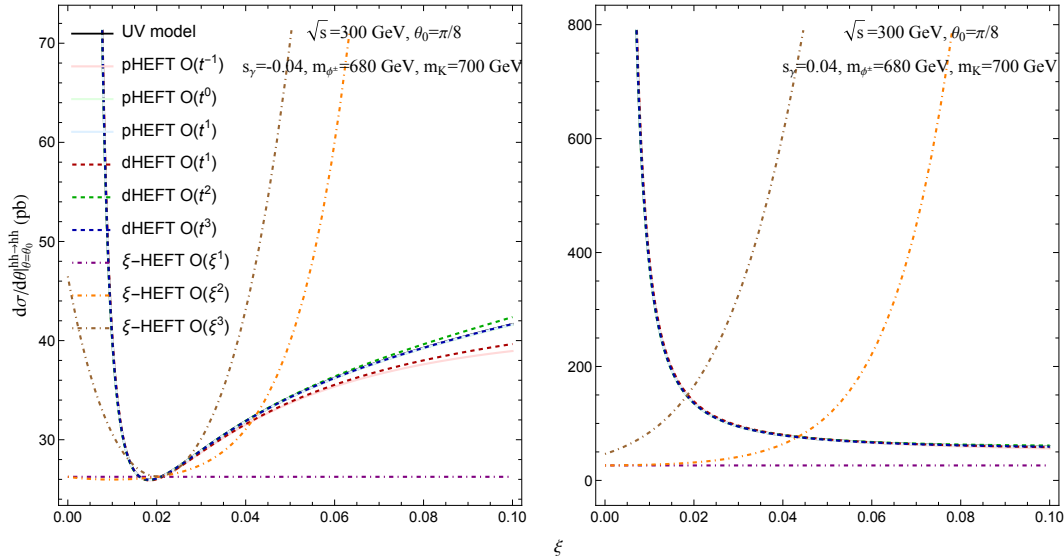


FIG. 6. Comparison between the UV model and the pHEFT and  $\xi$ -HEFT in the differential cross-section of  $hh \rightarrow hh$ , for a center-of-mass energy  $\sqrt{s} = 300$  GeV and a scattering angle  $\theta_0 = \pi/8$ . We set  $m_{\phi^\pm} = 680$  GeV, and  $m_K = 700$  GeV. The Higgs mass and electroweak vacuum expectation value are fixed to their experimentally measured values:  $m_h = 125$  GeV and  $v_{EW} = 246$  GeV. The left panel presents the case where  $s_\gamma = -0.04$ , while the right panel shows the case where  $s_\gamma = +0.04$ .

<sup>6</sup> The numerical results of the  $\xi$ -HEFT are obtained upon transforming  $\{Z_1, v_H\}$  into  $\{m_h, v_{EW}\}$ , allowing  $m_h$  and  $v_{EW}$  to be fixed by experimental values.

## D. $Y_2$ -HEFT vs. SMEFT

### 1. $Y_2$ -HEFT

In the standard UV-SMEFT matching [62, 63, 84], the Wilson coefficients of SMEFT are conventionally written as functions of the UV theory's parameters, specified in the unbroken (symmetric) phase,

$$\mathcal{P}_{Y_2} = \{Z_1, Z_2, Z_3, Y_1, Y_2, Y_3\}. \quad (50)$$

The power-counting scheme proceeds as an expansion in powers of  $1/Y_2^2$ , with  $Y_2^2$  denoting the real-triplet mass squared before electroweak symmetry breaking. Equivalently, the parameters follow the scaling:

$$Y_2\text{-HEFT: } Z_1 \sim Z_2 \sim Z_3 \sim Y_1 \sim Y_3 \sim \mathcal{O}(t^0), \quad Y_2^2 \sim \mathcal{O}(t^{-1}). \quad (51)$$

Within this power-counting scheme, one can derive a new HEFT, which we denote as the  $Y_2$ -HEFT.

As discussed above, the  $Y_2$ -HEFT Lagrangian follows directly from the pHEFT results via the substitutions listed below:

$$\begin{aligned} m_{\phi^\pm}^2 &\rightarrow Y_2^2 - \frac{Y_1^2 Z_3}{2Z_1} - \frac{Y_3^2 Y_1^2 (4Z_1 + Z_3)}{4Y_2^2 Z_1^2} + \mathcal{O}(Y_2^{-4}), \\ m_K^2 &\rightarrow Y_2^2 - \frac{Y_1^2 Z_3}{2Z_1} - \frac{Y_3^2 Y_1^2 (4Z_1 + Z_3)}{4Y_2^2 Z_1^2} + \mathcal{O}(Y_2^{-4}), \\ m_h^2 &\rightarrow -2Y_1^2 + \frac{Y_1^4 Y_3^2 (3Z_3 - 8Z_1)}{4Y_2^4 Z_1^2} + \mathcal{O}(Y_2^{-4}), \\ s_\gamma &\rightarrow -\frac{\sqrt{-Y_1^2} Y_3}{Y_2^2 \sqrt{Z_1}} - \frac{\sqrt{-Y_1^2} Y_3 (4Y_1^2 (Z_3 - 2Z_1) + Y_3^2)}{4Y_2^4 Z_1^{3/2}} + \mathcal{O}(Y_2^{-6}), \\ \xi &\rightarrow \frac{\sqrt{-Y_1^2} Y_3}{2Y_2^2 \sqrt{Z_1}} + \frac{\sqrt{-Y_1^2} Y_3 (2Y_1^2 Z_3 + Y_3^2)}{8Y_2^4 Z_1^{3/2}} + \mathcal{O}(Y_2^{-6}), \\ v_{\text{EW}} &\rightarrow \frac{\sqrt{-Y_1^2}}{\sqrt{Z_1}} + \frac{\sqrt{-Y_1^2} Y_3^2}{4Y_2^2 Z_1^{3/2}} + \frac{\sqrt{-Y_1^2} (2Y_1^2 Y_3^2 (3Z_3 - 8Z_1) + 3Y_3^4)}{32Y_2^4 Z_1^{5/2}} + \mathcal{O}(Y_2^{-6}), \end{aligned} \quad (52)$$

where the physical masses, the mixing angle  $s_\gamma$ , and the parameter  $\xi$  are expressed in terms of the Lagrangian couplings  $\{Z_i, Y_i\}$ . These relations are presented as a systematic expansion in  $1/Y_2^2$ , with only the first two leading orders explicitly shown. Note that  $-Y_1^2 > 0$  is required to ensure  $m_h \approx 125$  GeV remains at the electroweak scale, while  $m_{\phi^\pm}$  and  $m_K$  scale primarily with the large mass parameter  $Y_2^2$ .

## 2. SMEFT

We present the SMEFT matching Wilson coefficients in Tab. IV [62, 63, 84], where terms of  $\mathcal{O}(Y_2^{-8})$  and higher are neglected.

| dim-4           |   |
|-----------------|---|
| $C_{H^4}$       | $-Z_1 + \frac{Y_3^2}{2Y_2^2} + \frac{2Y_1^2Y_3^2}{Y_2^4} + \frac{6Y_1^4Y_3^2}{Y_2^6}$                             |
| dim-6           |   |
| $C_H$           | $\frac{Y_3^2}{2Y_2^4} \left[ (8Z_1 - Z_3) \left( 1 + \frac{4Y_1^2}{Y_2^2} \right) - \frac{4Y_3^2}{Y_2^2} \right]$ |
| $C_{HD}$        | $-\frac{2Y_3^2}{Y_2^4} \left( 1 + \frac{4Y_1^2}{Y_2^2} \right)$   |
| $C_{H\square}$  | $\frac{Y_3^2}{2Y_2^4} \left( 1 + \frac{4Y_1^2}{Y_2^2} \right)$  |
| dim-8           |   |
| $C_{H^8}$       | $\frac{Y_3^2}{2Y_2^6} (4Z_1 - Z_3)^2$   |
| $C_{H^6}^{(1)}$ | 0   |
| $C_{H^6}^{(2)}$ | $\frac{2Y_3^2}{Y_2^6} (-4Z_1 + Z_3)$  |
| $C_{H^4}^{(1)}$ | $\frac{4Y_3^2}{Y_2^6}$  |
| $C_{H^4}^{(3)}$ | $-\frac{2Y_3^2}{Y_2^6}$   |

TABLE IV. Dimension-6 and -8 Wilson coefficients of the bosonic operators resulting from the tree-level matching of the RHTM to the SMEFT.  $\mathcal{O}(1/Y_2^8)$  and higher orders are omitted here.  $C_{H^4}$  represents the coefficient of the Higgs doublet quartic interaction after matching.

As an illustration, we compute the momentum-independent trilinear and quartic Higgs couplings in order to compare SMEFT with  $Y_2$ -HEFT. After electroweak symmetry breaking, the Higgs doublet  $H$  is parameterized as:

$$H \rightarrow \begin{pmatrix} -iG^+ \\ \frac{v_T + h + iG^0}{\sqrt{2}} \end{pmatrix}, \quad (53)$$

where  $G^+, G^0$  denote the Goldstone bosons and  $v_T$  is the vacuum expectation value (VEV) determined by the tadpole condition of the Higgs boson. The electroweak VEV is obtained from  $m_W$  mass definition, which is given by

$$v_{\text{EW}}^2 = v_T^2 \left[ 1 + \frac{1}{4} v_T^4 \left( C_{H^6}^{(1)} - C_{H^6}^{(2)} \right) \right]. \quad (54)$$

In the unitary gauge, the scalar potential for the Higgs field  $h$  is :

$$V^{\text{SMEFT}}(h) = \frac{1}{2}Y_1^2(v_T + h)^2 - \frac{1}{4}C_{H^4}(v_T + h)^4 - \frac{1}{8}C_{H^6}(v_T + h)^6 - \frac{1}{16}C_{H^8}(v_T + h)^8, \quad (55)$$

while the kinetic part is:

$$\begin{aligned} \mathcal{L}_{\text{kin}}^{\text{SMEFT}}(h) &= \frac{1}{2}\mathcal{K}(h)\partial_\mu h\partial^\mu h, \\ \mathcal{K}(h) &= 1 + \frac{1}{2}(C_{HD} - 4C_{H\square})(v_T + h)^2 + \frac{1}{4}\left(C_{H^6}^{(1)} + C_{H^6}^{(2)}\right)(v_T + h)^4. \end{aligned} \quad (56)$$

After performing the field redefinition  $h' = \int_0^h \sqrt{\mathcal{K}(s)} ds$  to canonically normalize the kinetic term, we extract the triple and quartic Higgs self-couplings,  $\Delta\kappa_3$  and  $\Delta\kappa_4$  by the definition Eq. (2):

$$\begin{aligned} \Delta\kappa_3^{\text{SMEFT}} &= \frac{Y_1^2 Y_3^2 (2Z_1 - Z_3)}{2Z_1^2 Y_2^4} + \frac{Y_1^2 Y_3^4 (Z_1 - Z_3) + Y_1^4 Y_3^2 (9Z_1 Z_3 - 12Z_1^2 - 2Z_3^2)}{2Z_1^3 Y_2^6}, \\ \Delta\kappa_4^{\text{SMEFT}} &= \frac{Y_1^2 Y_3^2 (22Z_1 - 9Z_3)}{3Z_1^2 Y_2^4} + \frac{Y_1^2 Y_3^4 (11Z_1 - 9Z_3) + Y_1^4 Y_3^2 (123Z_1 Z_3 - 164Z_1^2 - 24Z_3^2)}{3Z_1^3 Y_2^6}, \end{aligned} \quad (57)$$

where higher-order terms in the  $1/Y_2^2$  expansion are neglected.

Notably, we find that up to  $\mathcal{O}(Y_2^{-6})$ , the results for  $\Delta\kappa_3^{\text{SMEFT}}$  and  $\Delta\kappa_4^{\text{SMEFT}}$  derived above are analytically identical to those obtained in the  $Y_2$ -HEFT. Although the two approaches follow different paths—one matching in the unbroken phase (SMEFT) and the other matching in the broken phase (pHEFT) followed by reparameterization and  $1/Y_2^2$  expansion—the resulting Higgs self-interactions are perfectly consistent. Thus, the hierarchical relation among the pHEFT,  $Y_2$ -HEFT, and the SMEFT can be expressed as

$$\text{pHEFT} \supset Y_2\text{-HEFT} \simeq \text{SMEFT}, \quad (58)$$

demonstrating that SMEFT emerges as a restricted limit within the broader HEFT framework in this example.

#### IV. THE PRIMARY HEFT OF OTHER UV MODELS

In the previous section, through matching the RHTM to various HEFTs and exploring their connections, we have shown that the primary HEFT serves as a foundational framework that can be used to derive other specific HEFTs, while generally provides the highest level of

perturbative accuracy. The idea of the primary HEFT is naturally applicable to other UV-HEFT matching procedures. In this section, we first formulate the primary HEFT within the  $Z_2$ -symmetric real singlet model (Z2RSM) and subsequently extend the discussion to the Two-Higgs Doublet Model (2HDM). The specific matching results for this model have been established in Ref. [72]; therefore, the present discussion is devoted exclusively to the construction of the primary HEFT and its foundational role.

## A. Z2RSM

### 1. Model Setup and Parameterization

In the  $Z_2$ -symmetric real singlet model (Z2RSM) [64, 65, 72, 80], the Standard Model  $SU(2)_L$  Higgs doublet is extended by a real singlet scalar field  $S$ , and a discrete  $Z_2$  symmetry is imposed under which  $S \rightarrow -S$ . The relevant part of the Lagrangian reads

$$\mathcal{L}_{\text{Z2RSM}} \supset (D^\mu H)^\dagger (D_\mu H) + \partial^\mu S \partial_\mu S - V(H, S), \quad (59)$$

$$V(H, S) = -\frac{\mu_1^2}{2} H^\dagger H - \frac{\mu_2^2}{2} S^2 + \frac{\lambda_1}{4} (H^\dagger H)^2 + \frac{\lambda_2}{4} S^4 + \frac{\lambda_3}{2} H^\dagger H S^2, \quad (60)$$

where the parameters  $\mu_i$  have mass dimension one, while the  $\lambda_i$  are dimensionless couplings.

After spontaneous symmetry breaking, the scalar fields are parametrized as

$$H = U \begin{pmatrix} 0 \\ \frac{1}{\sqrt{2}}(v_H + h_1) \end{pmatrix}, \quad S = \frac{1}{\sqrt{2}}(v_S + h_2), \quad (61)$$

where  $v_H$  and  $v_S$  denote the VEVs. They satisfy the minimization conditions of the scalar potential,

$$\mu_1^2 = \frac{1}{2} (\lambda_1 v_H^2 + \lambda_3 v_S^2), \quad \mu_2^2 = \frac{1}{2} (\lambda_3 v_H^2 + \lambda_2 v_S^2). \quad (62)$$

The physical Higgs mass eigenstates are obtained by a rotation with mixing angle  $\chi$ ,

$$\begin{pmatrix} h \\ K \end{pmatrix} = \begin{pmatrix} c_\chi & -s_\chi \\ s_\chi & c_\chi \end{pmatrix} \begin{pmatrix} h_1 \\ h_2 \end{pmatrix}, \quad (63)$$

where the mixing angle is given by

$$\tan(2\chi) = \frac{2\lambda_3 v_H v_S}{\lambda_2 v_S^2 - \lambda_1 v_H^2}, \quad (64)$$

and can be restricted to the range  $\chi \in [-\pi/4, \pi/4]$  without loss of generality.

The masses of the physical Higgs bosons are

$$M_{h,K}^2 = \frac{1}{4} \left[ \lambda_1 v_H^2 + \lambda_2 v_S^2 \mp \sqrt{(\lambda_1 v_H^2 - \lambda_2 v_S^2)^2 + 4\lambda_3^2 v_H^2 v_S^2} \right], \quad (65)$$

where  $h$  denotes the observed Higgs boson with mass  $m_h = 125$  GeV, and  $K$  is the heavier scalar state to be integrated out.

Expressed in terms of physical parameters, the scalar couplings can be written as

$$\begin{aligned} \lambda_1 &= \frac{2}{v_H^2} (M_K^2 s_\chi^2 + M_h^2 c_\chi^2), \\ \lambda_2 &= \frac{2}{v_S^2} (M_h^2 s_\chi^2 + M_K^2 c_\chi^2), \\ \lambda_3 &= \frac{2c_\chi s_\chi}{v_H v_S} (M_K^2 - M_h^2), \end{aligned} \quad (66)$$

where the linear dependence of the couplings  $\lambda_i$  on the heavy mass squared  $M_K^2$  is explicit.

## 2. Construction of the primary HEFT: parameter set and power counting

The Lagrangian contains five independent parameters, which can be reparameterized in terms of five physical quantities. To construct the primary HEFT, we choose the parameter set

$$(M_K, M_h, s_\chi, v_H, v_S), \quad (67)$$

together with the power-counting assignment

$$M_K \sim \mathcal{O}(t^{-1}), \quad M_h \sim s_\chi \sim v_H \sim v_S \sim \mathcal{O}(t^0). \quad (68)$$

From Eq. (66), one observes that the couplings  $\lambda_i$  depend linearly on the heavy mass squared  $M_K^2$ . As a result, no further expansion in inverse powers of  $M_K$  is required, and the interaction terms are kept exact. Consequently, the resulting primary HEFT preserves the maximal information from the underlying UV theory.

In contrast, if one adopts an alternative parameter set [72],

$$(M_K, M_h, s_\chi, v_H, \mu_2^2), \quad (69)$$

the numerical precision of the resulting EFT is compromised. This is because replacing  $v_S$  with  $\mu_2^2$  in the couplings  $\lambda_i$  introduces an additional dependence on  $M_K^2$ , necessitating

further expansions and truncations. From Eq. (66), we see that the couplings  $\lambda_i$  involve the structure  $1/v_S$ . Using the minimization conditions, this replacement is given by:

$$\frac{1}{v_S} \rightarrow \frac{c_\chi^2 M_K^2 + s_\chi^2 M_h^2 - \mu_2^2}{c_\chi s_\chi v_H (M_h^2 - M_K^2)}. \quad (70)$$

The right-hand side contains a factor of  $(M_h^2 - M_K^2)$  in the denominator. When performing an expansion in inverse powers of the heavy mass squared  $M_K^2$ , the term  $1/(M_h^2 - M_K^2)$  must be expanded and truncated. This process inevitably discards high-order contributions that are otherwise captured exactly when  $v_S$  is kept as an independent input. Consequently, the set  $(M_K, M_h, s_\chi, v_H, \mu_2^2)$  is not suitable for constructing the primary HEFT.

## B. 2HDM

### 1. General Basis vs. Higgs Basis

In the 2HDM [72, 83, 89] (for reviews, see e.g. Refs. [66, 67]), the Standard Model Higgs sector is enlarged by an additional  $SU(2)_L$  doublet. Unlike scalar extensions involving singlets, triplets, or other representations, the two-doublet structure possesses a global  $U(2)$  symmetry in the doublet space, reflecting the freedom to choose a basis for the Higgs fields. In a generic basis, the scalar Lagrangian is given by

$$\mathcal{L}_{\text{2HDM}} \supset (D_\mu \Phi_1)^\dagger (D^\mu \Phi_1) + (D_\mu \Phi_2)^\dagger (D^\mu \Phi_2) - V_{\text{2HDM}}, \quad (71)$$

$$\begin{aligned} V_{\text{2HDM}} = & m_{11}^2 \Phi_1^\dagger \Phi_1 + m_{22}^2 \Phi_2^\dagger \Phi_2 - m_{12}^2 (\Phi_1^\dagger \Phi_2 + \Phi_2^\dagger \Phi_1) + \frac{\lambda_1}{2} (\Phi_1^\dagger \Phi_1)^2 + \frac{\lambda_2}{2} (\Phi_2^\dagger \Phi_2)^2 \\ & + \lambda_3 (\Phi_1^\dagger \Phi_1) (\Phi_2^\dagger \Phi_2) + \lambda_4 (\Phi_1^\dagger \Phi_2) (\Phi_2^\dagger \Phi_1) + \frac{\lambda_5}{2} \left[ (\Phi_1^\dagger \Phi_2)^2 + (\Phi_2^\dagger \Phi_1)^2 \right], \end{aligned} \quad (72)$$

where a  $\mathbb{Z}_2$  symmetry ( $\Phi_1 \rightarrow \Phi_1$ ,  $\Phi_2 \rightarrow -\Phi_2$ ) is imposed and softly broken by the  $m_{12}^2$  term. We assume all parameters to be real, consistent with a CP-conserving scenario. The VEVs of  $\Phi_1$  and  $\Phi_2$  are denoted as  $v_1$  and  $v_2$ , respectively.

Another widely used basis is the Higgs basis  $\{H_1, H_2\}$ , where only one doublet acquires a non-zero VEV [90–93]. The transformation from the general basis to the Higgs basis is performed via a rotation by the angle  $\beta$ :

$$\begin{pmatrix} H_1 \\ H_2 \end{pmatrix} = \begin{pmatrix} c_\beta & s_\beta \\ -s_\beta & c_\beta \end{pmatrix} \begin{pmatrix} \Phi_1 \\ \Phi_2 \end{pmatrix}, \quad (73)$$

where  $t_\beta = v_2/v_1$  and  $v = \sqrt{v_1^2 + v_2^2} \approx 246 \text{ GeV}$ . In this basis, the scalar potential is parameterized as

$$\begin{aligned} V_{2\text{HDM}}^H = & Y_1 H_1^\dagger H_1 + Y_2 H_2^\dagger H_2 + (Y_3 H_1^\dagger H_2 + \text{h.c.}) \\ & + \frac{Z_1}{2} (H_1^\dagger H_1)^2 + \frac{Z_2}{2} (H_2^\dagger H_2)^2 + Z_3 (H_1^\dagger H_1) (H_2^\dagger H_2) + Z_4 (H_1^\dagger H_2) (H_2^\dagger H_1) \\ & + \left\{ \frac{Z_5}{2} (H_1^\dagger H_2)^2 + Z_6 (H_1^\dagger H_1) (H_1^\dagger H_2) + Z_7 (H_2^\dagger H_2) (H_1^\dagger H_2) + \text{h.c.} \right\}, \end{aligned} \quad (74)$$

where all  $Z_i$  and  $Y_i$  parameters are real. Note that while the Higgs basis potential contains 10 potential parameters ( $Y_{1,2,3}$  and  $Z_{1,\dots,7}$ ), the underlying  $\mathbb{Z}_2$  symmetry and the minimization conditions reduce the number of independent parameters. Specifically, only five of the  $Z_i$  couplings are independent due to the algebraic relations imposed by the basis transformation, leading to a total of eight independent parameters in the model.

## 2. Construction of the primary HEFT: parameter set and power counting

The construction of the primary HEFT starts with the choice of eight parameters, guided by the principle of selecting as many physical parameters as possible. However, in the 2HDM there are only seven physical parameters, namely  $m_h, m_H, m_A, m_{H^\pm}, v, t_\beta$ , and  $c_{\beta-\alpha}$ . Therefore, one additional parameter must be taken from the Lagrangian. A convenient choice is either  $Y_2$  in the Higgs basis (see Eq. (74)) or  $m_{12}$  in the general basis (see Eq. (72)).

We denote these two choices as

$$\text{Set 1: } (m_h, m_H, m_A, m_{H^\pm}, v, t_\beta, c_{\beta-\alpha}, Y_2), \quad (75)$$

$$\text{Set 2: } (m_h, m_H, m_A, m_{H^\pm}, v, t_\beta, c_{\beta-\alpha}, m_{12}), \quad (76)$$

where  $h$  denotes the light Higgs boson,  $H$  the heavy CP-even Higgs boson,  $A$  the heavy CP-odd Higgs boson, and  $H^\pm$  the heavy charged Higgs bosons. Here  $v \equiv \sqrt{v_1^2 + v_2^2}$ , and  $\alpha$  denotes the mixing angle between the two neutral CP-even scalar fields.

Adopting Set 1, the remaining parameters in the Higgs-basis potential are determined as:

$$\begin{aligned}
Y_1 &= -\frac{Z_1}{2}v^2, \quad Y_3 = -\frac{Z_6}{2}v^2, \\
Z_1 &= \frac{s_{\beta-\alpha}^2 m_h^2 + c_{\beta-\alpha}^2 m_H^2}{v^2}, \\
Z_2 &= \frac{1}{2v^2 t_\beta^3} \left[ c_{\beta-\alpha}^2 t_\beta (3t_\beta^4 - 8t_\beta^2 + 3) (m_h^2 - m_H^2) + 2t_\beta (t_\beta^2 - 1)^2 (m_H^2 - Y_2) \right. \\
&\quad \left. - m_h^2 (t_\beta^5 - 4t_\beta^3 + t_\beta) + s_{\beta-\alpha} c_{\beta-\alpha} (t_\beta^6 - 7t_\beta^4 + 7t_\beta^2 - 1) (m_h^2 - m_H^2) \right], \\
Z_3 &= \frac{2}{v^2} (m_{H^\pm}^2 - Y_2), \\
Z_4 &= \frac{c_{\beta-\alpha}^2 (m_h^2 - m_H^2) + m_A^2 + m_H^2 - 2m_{H^\pm}^2}{v^2}, \\
Z_5 &= \frac{c_{\beta-\alpha}^2 (m_h^2 - m_H^2) - m_A^2 + m_H^2}{v^2}, \\
Z_6 &= \frac{c_{\beta-\alpha} s_{\beta-\alpha} (m_h^2 - m_H^2)}{v^2}, \\
Z_7 &= \frac{1}{2v^2 t_\beta^2} \left[ -3c_{\beta-\alpha}^2 t_\beta (t_\beta^2 - 1) (m_h^2 - m_H^2) + t_\beta (t_\beta^2 - 1) (m_h^2 - 2m_H^2 + 2Y_2) \right. \\
&\quad \left. - s_{\beta-\alpha} c_{\beta-\alpha} (t_\beta^4 - 4t_\beta^2 + 1) (m_h^2 - m_H^2) \right]. \tag{77}
\end{aligned}$$

From these expressions, we observe that the squared masses of the heavy states, such as  $m_H^2$ ,  $m_A^2$ , and  $m_{H^\pm}^2$ , appear only in the numerator. As a result, after integrating out the heavy propagators, no additional expansion in inverse powers of the heavy masses is required. Set 1 is well-suited for constructing the primary HEFT. Its power counting is defined as:

$$m_H \sim m_A \sim m_{H^\pm} \sim \mathcal{O}(t^{-1}), \quad m_h \sim v \sim t_\beta \sim c_{\beta-\alpha} \sim Y_2 \sim \mathcal{O}(t^0), \tag{78}$$

where only the heavy masses scale as  $\mathcal{O}(t^{-1})$ , while the remaining parameters, including  $Y_2$ , are treated as  $\mathcal{O}(t^0)$  and kept independent of the heavy scale.

To evaluate whether Set 2 is also suitable, we examine the relation between  $Y_2$  and  $m_{12}^2$ . Using the minimization conditions,  $Y_2$  can be expressed in terms of the parameters in Set 2 as:

$$Y_2 = \frac{m_{12}^2}{s_\beta c_\beta} - \frac{1}{2} (s_{\beta-\alpha}^2 m_h^2 + c_{\beta-\alpha}^2 m_H^2) - (m_h^2 - m_H^2) s_{\beta-\alpha} c_{\beta-\alpha} \cot(2\beta). \tag{79}$$

In this expression, the heavy mass squared  $m_H^2$  appears exclusively in the numerator. Unlike the Z2RSM case where the replacement of  $v_S$  by  $\mu_2^2$  introduced inverse powers of the heavy mass (as seen in Eq. (70)), switching from  $Y_2$  to  $m_{12}^2$  in the 2HDM does not necessitate

any additional expansion in  $1/m_H^2$ . Consequently, Set 2 is also suitable for constructing a primary HEFT, as it maintains the exact linear structure required for a precise matching.

## V. CONCLUSION AND DISCUSSION

In this work, we reanalyze the matching between the RHTM and the HEFT for various parameter sets and power counting schemes. For the first time, we obtain the complete HEFT matching results, including fermionic operators. We have established the concept of a primary Higgs Effective Field Theory (pHEFT) as a foundational and maximally precise benchmark for matching UV completions to the HEFT framework via observing the standard matching method almost based on an expansion of the effective propagators of the heavy states. We demonstrate that by choosing a parameter set consisting of physical masses, mixing angles, and vacuum expectation values—and adopting a power-counting scheme that expands solely in inverse powers of the heavy masses—we obtain an effective theory that retains the complete dynamical information from the UV completion at a given order.

The primary HEFT serves as a master framework from which other, more restricted HEFTs can be systematically derived through parameter mappings and the imposition of additional scaling rules. We explicitly mapped the pHEFT to several specific cases:

- The decoupling HEFT (dHEFT), obtained by treating the mixing angle  $s_\gamma$  and VEV ratio  $\xi$  as suppressed quantities.
- The  $\xi$ -HEFT, recovered by applying a reparametrization and  $\xi$ -expansion to the pHEFT, with the decoupling limit being implicitly implemented.
- The  $Z_2$ -HEFT, a formulation based on the parameter set  $\{m_{\phi^\pm}^2, m_K^2, m_h, v_{\text{EW}}, Z_2, \xi\}$  where the mixing angle  $s_\gamma$  is expressed in terms of the UV Lagrangian coupling  $Z_2$ . This case is particularly instructive, as it highlights that not all parameter sets are created “equal”. Constructing the  $Z_2$ -HEFT requires an additional inverse-mass expansion, which inherently introduces truncation errors and makes it less precise than the pHEFT. This comparison underscores a central finding: A well-defined primary HEFT should be constructed in a parameter basis in which the UV Lagrangian parameters depend polynomially, with non-negative powers, on the heavy masses, thereby avoiding such secondary expansions.

- The  $Y_2$ -HEFT, derived from the pHEFT via a reparameterization into SMEFT variables followed by an expansion in the Lagrangian mass parameters, reproduces the SMEFT predictions. This explicitly shows that SMEFT arises as a nested limit of HEFT.

A key result is the hierarchical embedding among these EFTs: pHEFT  $\supset$  dHEFT  $\supset$   $\xi$ -HEFT. This structure proves that the computationally intensive step of integrating out heavy degrees of freedom via a functional or diagrammatic matching needs to be performed only once to obtain the pHEFT. Phenomenologically motivated EFT limits can be accessed through straightforward algebraic rescalings and truncations of the pHEFT Lagrangian, thereby avoiding redundant matching calculations. We should emphasize that this concept has clear precedents, and a key takeaway for students is that expansion series are generally “non-commutative”—a fundamental lesson for undergraduate studies <sup>7</sup>.

We further generalize the primary HEFT idea to other UV models with scalar extensions, namely the  $Z_2$ -symmetric real singlet model and the two-Higgs doublet model. The analysis, reinforced by the lessons from the  $Z_2$ -HEFT, led to clear criteria for selecting an optimal parameter set: a “good” primary HEFT is characterized by linear relations between heavy masses and the original UV Lagrangian couplings. This linearity ensures that no secondary expansion is necessary when integrating out heavy fields, preserving maximal UV information and numerical precision. Parameter sets that introduce non-linear relations (like the  $Z_2$ -based set) inevitably require additional inverse-mass expansions, leading to a loss of accuracy and making them unsuitable as a primary benchmark.

In summary, the primary HEFT formalism provides a unified, efficient, and precision-oriented strategy for top-down EFT matching. It clarifies the connections between various low-energy effective descriptions arising from the same UV physics and establishes a reliable benchmark for assessing the truncation errors introduced by more restrictive power-counting schemes. This work paves the way for more systematic, automated, and accurate interpretations of high-energy physics in the context of Higgs effective field theory.

---

<sup>7</sup> Here, we use the term “non-commutative” in a practical sense: results derived under less restrictive parameter assumptions cannot be fully recovered from results obtained under stricter ones.

## Appendix A: Solutions for the Heavy Fields in the pHEFT

In this section, we present the solutions for the heavy fields that lead to the primary HEFT, which are given below.

$$\begin{aligned}
K_0 = & -\frac{h^2}{2\xi(4\xi^2+1)v_H m_K^2} \left\{ -c_\gamma^3 \left[ (4\xi^2+1)m_K^2 - 3m_{\phi^\pm}^2 \right] + c_\gamma \left[ (4\xi^2+1)m_K^2 - 3m_{\phi^\pm}^2 \right] \right. \\
& \left. + \xi c_\gamma^2 s_\gamma \left[ (4\xi^2+1)m_K^2 - 6m_{\phi^\pm}^2 \right] + 2\xi m_{\phi^\pm}^2 s_\gamma \right\} + \mathcal{O}(h^3), \\
\phi_{10} = \phi_{20} = & 0, \\
K_1 = & \frac{c_\gamma \langle V_\mu \sigma_3 \rangle \langle V^\mu \sigma_3 \rangle}{(4\xi^2+1)m_K^4} \left\{ (4\xi^2+1)\xi v_H m_K^2 \right. \\
& + h \left[ s_\gamma \left( (4\xi^2+1)(2c_\gamma^2-1)m_K^2 - 3c_\gamma^2 m_{\phi^\pm}^2 \right) + 2\xi c_\gamma \left( (2-3c_\gamma^2)m_{\phi^\pm}^2 - (4\xi^2+1)m_K^2 s_\gamma^2 \right) \right] \} \\
& + \frac{\langle V_\mu V^\mu \rangle}{2m_K^4} \left\{ -v_H m_K^2 (4\xi c_\gamma + s_\gamma) + \frac{hc_\gamma}{\xi(4\xi^2+1)} \left[ \xi s_\gamma \left( 2(9c_\gamma^2-2)m_{\phi^\pm}^2 - 5(4\xi^2+1)(2c_\gamma^2-1)m_K^2 \right) \right. \right. \\
& \left. \left. + c_\gamma \left( m_{\phi^\pm}^2 (3(8\xi^2-1)c_\gamma^2 - 16\xi^2 + 3) + 2(16\xi^4-1)m_K^2 s_\gamma^2 \right) \right] \right\} + \mathcal{O}(h^2) \\
& + \bar{Q}_L U \begin{pmatrix} y_u & 0 \\ 0 & y_d \end{pmatrix} Q_R \times \frac{-s_\gamma}{\sqrt{2}\xi(4\xi^2+1)v_H m_K^4} \left\{ (4\xi^2+1)\xi v_H m_K^2 \right. \\
& \left. + hc_\gamma \left[ 2(4\xi^2+1)m_K^2 (\xi c_\gamma^2 + c_\gamma s_\gamma - \xi) + m_{\phi^\pm}^2 (-6\xi c_\gamma^2 - 3c_\gamma s_\gamma + 4\xi) \right] \right\} + \text{h.c.}, \\
\phi_{11} = & \frac{\xi v_H \langle V_\mu \sigma_1 \rangle \langle V^\mu \sigma_3 \rangle + 2i \langle V_\mu \sigma_2 \rangle D^\mu h (\xi c_\gamma + s_\gamma)}{(4\xi^2+1)m_{\phi^\pm}^2} \\
& + \frac{ih(\xi c_\gamma + s_\gamma)}{(4\xi^2+1)^2 m_{\phi^\pm}^2} \left[ (4\xi^2+1) \langle D_\mu V^\mu \sigma_2 \rangle + 2i \langle V_\mu \sigma_1 \rangle \langle V^\mu \sigma_3 \rangle \right] + \mathcal{O}(h^2) \\
& + \bar{Q}_L U \begin{pmatrix} 0 & -y_d \\ y_u & 0 \end{pmatrix} Q_R \times \frac{\sqrt{2} \left\{ (4\xi^2+1)\xi v_H + h[(4\xi^2-1)s_\gamma - 2\xi c_\gamma] \right\}}{(4\xi^2+1)^2 v_H m_{\phi^\pm}^2} + \text{h.c.}, \\
\phi_{21} = & \frac{\xi v_H \langle V_\mu \sigma_2 \rangle \langle V^\mu \sigma_3 \rangle - 2i \langle V_\mu \sigma_1 \rangle D^\mu h (\xi c_\gamma + s_\gamma)}{(4\xi^2+1)m_{\phi^\pm}^2} \\
& - \frac{ih(\xi c_\gamma + s_\gamma)}{(4\xi^2+1)^2 m_{\phi^\pm}^2} \left[ (4\xi^2+1) \langle D_\mu V^\mu \sigma_1 \rangle - 2i \langle V_\mu \sigma_2 \rangle \langle V^\mu \sigma_3 \rangle \right] + \mathcal{O}(h^2) \\
& + \bar{Q}_L U \begin{pmatrix} 0 & iy_d \\ iy_u & 0 \end{pmatrix} Q_R \times \frac{\sqrt{2} \left\{ (4\xi^2+1)\xi v_H + h[(4\xi^2-1)s_\gamma - 2\xi c_\gamma] \right\}}{(4\xi^2+1)^2 v_H m_{\phi^\pm}^2} + \text{h.c.}, \tag{A1}
\end{aligned}$$

Here the solutions are further expanded around the Higgs field  $h$  and  $V_\mu \equiv U^\dagger D_\mu U$ . The fields  $\phi_1$  and  $\phi_2$  vanish at lower orders and first acquire nonzero contributions at  $\mathcal{O}(t^1)$ . The custodial-symmetry-breaking structure  $\langle V_\mu \sigma_3 \rangle \langle V^\mu \sigma_3 \rangle$  first appears in the solution for

$K_1$ . The fields  $\phi_{11}$  and  $\phi_{21}$  exhibit similar structures, as they correspond to the real and imaginary components of the charged scalar field, respectively.

## Appendix B: EoM of $U$

When reducing operators to a complete basis, one frequently encounters terms containing  $D_\mu D^\mu U$ , which must be eliminated in favor of other operators using the equation of motion (EoM) of  $U$ . We present the corresponding derivation below.

Starting from a leading-order Lagrangian of the general form

$$\mathcal{L}^{\text{LO}} = a(h) \langle V_\mu \sigma_3 \rangle \langle V^\mu \sigma_3 \rangle + b(h) \langle V_\mu V^\mu \rangle + \frac{1}{2} D_\mu h D^\mu h - V(h),$$

where  $V_\mu \equiv U^\dagger D_\mu U$ ,  $a(h)$  and  $b(h)$  are polynomials in  $h$ , which we will henceforth denote simply as  $a$  and  $b$ . We solve the EoM for  $U$ ,

$$\frac{\partial \mathcal{L}^{\text{LO}}}{\partial U} = D_\mu \frac{\partial \mathcal{L}^{\text{LO}}}{\partial (D_\mu U)}, \quad (\text{B1})$$

which leads to

$$\begin{aligned} D_\mu D^\mu U = & -D_\mu U D^\mu U^\dagger U - \frac{D_\mu b}{b} D^\mu U - \frac{D_\mu a}{b} \langle V^\mu \sigma_3 \rangle U \sigma_3 \\ & - \frac{a}{b} \left[ D_\mu \langle V^\mu \sigma_3 \rangle U \sigma_3 + \langle V^\mu \sigma_3 \rangle D_\mu U \sigma_3 - \langle V_\mu \sigma_3 \rangle U \sigma_3 V^\mu \right], \end{aligned} \quad (\text{B2})$$

where on the right side there exists

$$D_\mu \langle V^\mu \sigma_3 \rangle = \langle D_\mu U^\dagger D^\mu U \sigma_3 \rangle + \langle U^\dagger \mathbf{D}_\mu \mathbf{D}^\mu \mathbf{U} \sigma_3 \rangle. \quad (\text{B3})$$

By combining the above two equations, we finally obtain

$$D_\mu \langle V^\mu \sigma_3 \rangle = -\frac{D_\mu (b + 2a)}{b + 2a} \langle V^\mu \sigma_3 \rangle. \quad (\text{B4})$$

Similarly, for the other two components of  $V^\mu$  we have

$$D_\mu \langle V^\mu \sigma_1 \rangle = -\frac{D_\mu b}{b} \langle V^\mu \sigma_1 \rangle - 2i \frac{a}{b} \langle V_\mu \sigma_2 \rangle \langle V^\mu \sigma_3 \rangle \quad (\text{B5})$$

$$D_\mu \langle V^\mu \sigma_2 \rangle = -\frac{D_\mu b}{b} \langle V^\mu \sigma_2 \rangle + 2i \frac{a}{b} \langle V_\mu \sigma_1 \rangle \langle V^\mu \sigma_3 \rangle \quad (\text{B6})$$

## ACKNOWLEDGMENTS

X.W. thanks Fengkun Guo and Jiannan Ding for helpful discussions. The work of H.S. is partially supported by IBS under the project code, IBS-R018-D1. X.W. is supported by the National Science Foundation of China under Grants No. 11947416.

---

- [1] S. Chatrchyan *et al.* (CMS), Observation of a New Boson at a Mass of 125 GeV with the CMS Experiment at the LHC, *Phys. Lett. B* **716**, 30 (2012), arXiv:1207.7235 [hep-ex].
- [2] G. Aad *et al.* (ATLAS), Observation of a new particle in the search for the Standard Model Higgs boson with the ATLAS detector at the LHC, *Phys. Lett. B* **716**, 1 (2012), arXiv:1207.7214 [hep-ex].
- [3] A. Hayrapetyan *et al.* (CMS), Search for heavy neutral Higgs bosons A and H in the  $t\bar{t}^-Z$  channel in proton-proton collisions at 13 TeV, *Phys. Lett. B* **866**, 139568 (2025), arXiv:2412.00570 [hep-ex].
- [4] G. Aad *et al.* (ATLAS), Search for R-parity violating supersymmetric decays of the top squark to a b-jet and a lepton in  $s=13$  TeV pp collisions with the ATLAS detector, *Phys. Rev. D* **110**, 092004 (2024), arXiv:2406.18367 [hep-ex].
- [5] S. Weinberg, Effective Gauge Theories, *Phys. Lett. B* **91**, 51 (1980).
- [6] H. Georgi, Effective field theory, *Annual Review of Nuclear and Particle Science* **43**, 209 (1993).
- [7] S. Weinberg, Baryon and Lepton Nonconserving Processes, *Phys. Rev. Lett.* **43**, 1566 (1979).
- [8] W. Buchmuller and D. Wyler, Effective Lagrangian Analysis of New Interactions and Flavor Conservation, *Nucl. Phys. B* **268**, 621 (1986).
- [9] C. N. Leung, S. T. Love, and S. Rao, Low-Energy Manifestations of a New Interaction Scale: Operator Analysis, *Z. Phys. C* **31**, 433 (1986).
- [10] I. Brivio and M. Trott, The Standard Model as an Effective Field Theory, *Phys. Rept.* **793**, 1 (2019), arXiv:1706.08945 [hep-ph].
- [11] T. Appelquist and C. W. Bernard, Strongly Interacting Higgs Bosons, *Phys. Rev. D* **22**, 200 (1980).
- [12] A. C. Longhitano, Heavy Higgs Bosons in the Weinberg-Salam Model, *Phys. Rev. D* **22**, 1166 (1980).

- [13] A. C. Longhitano, Low-Energy Impact of a Heavy Higgs Boson Sector, *Nucl. Phys. B* **188**, 118 (1981).
- [14] F. Feruglio, The Chiral approach to the electroweak interactions, *Int. J. Mod. Phys. A* **8**, 4937 (1993), arXiv:hep-ph/9301281.
- [15] M. J. Herrero and E. Ruiz Morales, The Electroweak chiral Lagrangian for the Standard Model with a heavy Higgs, *Nucl. Phys. B* **418**, 431 (1994), arXiv:hep-ph/9308276.
- [16] M. J. Herrero and E. Ruiz Morales, Nondecoupling effects of the SM higgs boson to one loop, *Nucl. Phys. B* **437**, 319 (1995), arXiv:hep-ph/9411207.
- [17] B. Grinstein and M. Trott, A Higgs-Higgs bound state due to new physics at a TeV, *Phys. Rev. D* **76**, 073002 (2007), arXiv:0704.1505 [hep-ph].
- [18] G. Buchalla and O. Cata, Effective Theory of a Dynamically Broken Electroweak Standard Model at NLO, *JHEP* **07**, 101, arXiv:1203.6510 [hep-ph].
- [19] R. Alonso, M. B. Gavela, L. Merlo, S. Rigolin, and J. Yepes, The Effective Chiral Lagrangian for a Light Dynamical "Higgs Particle", *Phys. Lett. B* **722**, 330 (2013), [Erratum: *Phys.Lett.B* 726, 926 (2013)], arXiv:1212.3305 [hep-ph].
- [20] G. Buchalla, O. Catà, and C. Krause, Complete Electroweak Chiral Lagrangian with a Light Higgs at NLO, *Nucl. Phys. B* **880**, 552 (2014), [Erratum: *Nucl.Phys.B* 913, 475–478 (2016)], arXiv:1307.5017 [hep-ph].
- [21] I. Brivio, T. Corbett, O. J. P. Éboli, M. B. Gavela, J. Gonzalez-Fraile, M. C. Gonzalez-Garcia, L. Merlo, and S. Rigolin, Disentangling a dynamical Higgs, *JHEP* **03**, 024, arXiv:1311.1823 [hep-ph].
- [22] G. Buchalla, O. Catá, and C. Krause, On the Power Counting in Effective Field Theories, *Phys. Lett. B* **731**, 80 (2014), arXiv:1312.5624 [hep-ph].
- [23] M. B. Gavela, J. Gonzalez-Fraile, M. C. Gonzalez-Garcia, L. Merlo, S. Rigolin, and J. Yepes, CP violation with a dynamical Higgs, *JHEP* **10**, 044, arXiv:1406.6367 [hep-ph].
- [24] A. Pich, I. Rosell, J. Santos, and J. J. Sanz-Cillero, Low-energy signals of strongly-coupled electroweak symmetry-breaking scenarios, *Phys. Rev. D* **93**, 055041 (2016), arXiv:1510.03114 [hep-ph].
- [25] R. Alonso, E. E. Jenkins, and A. V. Manohar, A Geometric Formulation of Higgs Effective Field Theory: Measuring the Curvature of Scalar Field Space, *Phys. Lett. B* **754**, 335 (2016), arXiv:1511.00724 [hep-ph].

[26] I. Brivio, J. Gonzalez-Fraile, M. C. Gonzalez-Garcia, and L. Merlo, The complete HEFT Lagrangian after the LHC Run I, *Eur. Phys. J. C* **76**, 416 (2016), arXiv:1604.06801 [hep-ph].

[27] R. Alonso, E. E. Jenkins, and A. V. Manohar, Geometry of the Scalar Sector, *JHEP* **08**, 101, arXiv:1605.03602 [hep-ph].

[28] A. Pich, I. Rosell, J. Santos, and J. J. Sanz-Cillero, Fingerprints of heavy scales in electroweak effective Lagrangians, *JHEP* **04**, 012, arXiv:1609.06659 [hep-ph].

[29] L. Merlo, S. Saa, and M. Sacristán-Barbero, Baryon Non-Invariant Couplings in Higgs Effective Field Theory, *Eur. Phys. J. C* **77**, 185 (2017), arXiv:1612.04832 [hep-ph].

[30] A. Pich, Effective Field Theory with Nambu-Goldstone Modes, in *Effective Field Theory in Particle Physics and Cosmology*, Lecture Notes of the Les Houches Summer School, Vol. 108, edited by S. Davidson, P. Gambino, M. Laine, M. Neubert, and C. Salomon (Oxford University Press, 2019) p. 3, arXiv:1804.05664 [hep-ph].

[31] C. Krause, A. Pich, I. Rosell, J. Santos, and J. J. Sanz-Cillero, Colorful Imprints of Heavy States in the Electroweak Effective Theory, *JHEP* **05**, 092, arXiv:1810.10544 [hep-ph].

[32] H. Sun, M.-L. Xiao, and J.-H. Yu, Complete NLO operators in the Higgs effective field theory, *JHEP* **05**, 043, arXiv:2206.07722 [hep-ph].

[33] H. Sun, M.-L. Xiao, and J.-H. Yu, Complete NNLO operator bases in Higgs effective field theory, *JHEP* **04**, 086, arXiv:2210.14939 [hep-ph].

[34] A. Falkowski and R. Rattazzi, Which EFT, *JHEP* **10**, 255, arXiv:1902.05936 [hep-ph].

[35] I. Brivio, SMEFTsim 3.0 — a practical guide, *JHEP* **04**, 073, arXiv:2012.11343 [hep-ph].

[36] J. J. Ethier, G. Magni, F. Maltoni, L. Mantani, E. R. Nocera, J. Rojo, E. Slade, E. Vryonidou, and C. Zhang (SMEFiT), Combined SMEFT interpretation of Higgs, diboson, and top quark data from the LHC, *JHEP* **11**, 089, arXiv:2105.00006 [hep-ph].

[37] B. Grzadkowski, M. Iskrzyński, M. Misiak, and J. Rosiek, Dimension-six terms in the standard model lagrangian, *JHEP* **10** (085), arXiv:1008.4884 [hep-ph].

[38] C. W. Murphy, Dimension-8 operators in the standard model effective field theory, *JHEP* **10** (174), arXiv:2005.00059 [hep-ph].

[39] Z. Ren and J.-H. Yu, A complete set of the dimension-8 Green's basis operators in the Standard Model effective field theory, *JHEP* **02**, 134, arXiv:2211.01420 [hep-ph].

[40] B. Henning, X. Lu, T. Melia, and H. Murayama, 2, 84, 30, 993, 560, . . .: Higher dimension operators in the sm eft, *JHEP* **08** (016), arXiv:1512.03433 [hep-th].

- [41] B. Henning, X. Lu, and H. Murayama, How to use the Standard Model effective field theory, *JHEP* **01**, 023, arXiv:1412.1837 [hep-ph].
- [42] G. Isidori, F. Wilsch, and D. Wyler, The standard model effective field theory at work, *Rev. Mod. Phys.* **96**, 015006 (2024), arXiv:2303.16922 [hep-ph].
- [43] J. Gargalionis, J. Quevillon, P. N. H. Vuong, and T. You, Linear Standard Model extensions in the SMEFT at one loop and Tera-Z, *JHEP* **07**, 136, arXiv:2412.01759 [hep-ph].
- [44] T. Cohen, N. Craig, X. Lu, and D. Sutherland, Is SMEFT Enough?, *JHEP* **03**, 237, arXiv:2008.08597 [hep-ph].
- [45] I. Banta, T. Cohen, N. Craig, X. Lu, and D. Sutherland, Non-decoupling new particles, *JHEP* **02**, 029, arXiv:2110.02967 [hep-ph].
- [46] G. N. Remmen and N. L. Rodd, Positively Identifying HEFT or SMEFT (2024), arXiv:2412.07827 [hep-ph].
- [47] L. Gráf, B. Henning, X. Lu, T. Melia, and H. Murayama, Hilbert series, the Higgs mechanism, and HEFT, *JHEP* **02**, 064, arXiv:2211.06275 [hep-ph].
- [48] R. Gómez-Ambrosio, F. J. Llanes-Estrada, A. Salas-Bernárdez, and J. J. Sanz-Cillero, SMEFT is falsifiable through multi-Higgs measurements (even in the absence of new light particles), *Commun. Theor. Phys.* **75**, 095202 (2023), arXiv:2207.09848 [hep-ph].
- [49] R. Gómez-Ambrosio, F. J. Llanes-Estrada, A. Salas-Bernárdez, and J. J. Sanz-Cillero, Distinguishing electroweak EFTs with  $WLWL \rightarrow n \times h$ , *Phys. Rev. D* **106**, 053004 (2022), arXiv:2204.01763 [hep-ph].
- [50] R. Alonso and M. West, Roads to the Standard Model, *Phys. Rev. D* **105**, 096028 (2022), arXiv:2109.13290 [hep-ph].
- [51] I. n. Asiáin, D. Espriu, and F. Mescia, Introducing tools to test Higgs boson interactions via WW scattering: One-loop calculations and renormalization in the Higgs effective field theory, *Phys. Rev. D* **105**, 015009 (2022), arXiv:2109.02673 [hep-ph].
- [52] T. Cohen, N. Craig, X. Lu, and D. Sutherland, Unitarity violation and the geometry of Higgs EFTs, *JHEP* **12**, 003, arXiv:2108.03240 [hep-ph].
- [53] M. J. Herrero and R. A. Morales, One-loop renormalization of vector boson scattering with the electroweak chiral Lagrangian in covariant gauges, *Phys. Rev. D* **104**, 075013 (2021), arXiv:2107.07890 [hep-ph].

[54] M. J. Herrero and R. A. Morales, One-loop corrections for WW to HH in Higgs EFT with the electroweak chiral Lagrangian, *Phys. Rev. D* **106**, 073008 (2022), arXiv:2208.05900 [hep-ph].

[55] L. Alasfar *et al.*, Effective Field Theory descriptions of Higgs boson pair production, *SciPost Phys. Comm. Rep.* **2024**, 2 (2024), arXiv:2304.01968 [hep-ph].

[56] H. T. Li, Z.-G. Si, J. Wang, X. Zhang, and D. Zhao, QCD corrections to Higgs boson pair production and decay to the  $bb^-\tau^+\tau^-$  final state, *Phys. Lett. B* **868**, 139776 (2025), arXiv:2503.22001 [hep-ph].

[57] J.-L. Ding *et al.*, Constraining the Higgs potential using multi-Higgs production (2026), arXiv:2601.13248 [hep-ph].

[58] I. Brivio, R. Gröber, and K. Schmid, The Art of Counting: a reappraisal of the HEFT expansion (2025), arXiv:2511.23410 [hep-ph].

[59] I. Brivio, R. Gröber, and K. Schmid, Higgs pair production in gluon fusion to higher orders in Higgs Effective Field Theory (2025), arXiv:2511.23411 [hep-ph].

[60] R. Alonso, C. Englert, W. Naskar, and S. U. Rahaman, Assessing (H)EFT theory errors by pitting EoM against Field Redefinitions (2025), arXiv:2511.15609 [hep-ph].

[61] R. Alonso, S. Chattopadhyay, and J. Ingoldby, The Potential of HEFT and the scale of New Physics (2025), arXiv:2512.13612 [hep-ph].

[62] J. Ellis, K. Mimasu, and F. Zampedri, Dimension-8 SMEFT analysis of minimal scalar field extensions of the Standard Model, *JHEP* **10**, 051, arXiv:2304.06663 [hep-ph].

[63] T. Corbett, A. Helset, A. Martin, and M. Trott, EWPD in the SMEFT to dimension eight, *JHEP* **06**, 076, arXiv:2102.02819 [hep-ph].

[64] T. Robens and T. Stefaniak, Status of the Higgs Singlet Extension of the Standard Model after LHC Run 1, *Eur. Phys. J. C* **75**, 104 (2015), arXiv:1501.02234 [hep-ph].

[65] T. Robens and T. Stefaniak, LHC Benchmark Scenarios for the Real Higgs Singlet Extension of the Standard Model, *Eur. Phys. J. C* **76**, 268 (2016), arXiv:1601.07880 [hep-ph].

[66] J. F. Gunion, H. E. Haber, G. L. Kane, and S. Dawson, *The Higgs Hunter's Guide*, Vol. 80 (2000).

[67] G. C. Branco, P. M. Ferreira, L. Lavoura, M. N. Rebelo, M. Sher, and J. P. Silva, Theory and phenomenology of two-Higgs-doublet models, *Phys. Rept.* **516**, 1 (2012), arXiv:1106.0034 [hep-ph].

[68] J. C. Criado, MatchingTools: a Python library for symbolic effective field theory calculations, *Comput. Phys. Commun.* **227**, 42 (2018), arXiv:1710.06445 [hep-ph].

[69] S. Das Bakshi, J. Chakrabortty, and S. K. Patra, CoDEx: Wilson coefficient calculator connecting SMEFT to UV theory, *Eur. Phys. J. C* **79**, 21 (2019), arXiv:1808.04403 [hep-ph].

[70] J. Fuentes-Martín, M. König, J. Pagès, A. E. Thomsen, and F. Wilsch, A proof of concept for matchete: an automated tool for matching effective theories, *Eur. Phys. J. C* **83**, 662 (2023), arXiv:2212.04510 [hep-ph].

[71] A. Carmona, A. Lazopoulos, P. Olgoso, and J. Santiago, Matchmakereft: automated tree-level and one-loop matching, *SciPost Phys.* **12**, 198 (2022), arXiv:2112.10787 [hep-ph].

[72] S. Dawson, D. Fontes, C. Quezada-Calonge, and J. J. Sanz-Cillero, Is the HEFT matching unique?, *Phys. Rev. D* **109**, 055037 (2024), arXiv:2311.16897 [hep-ph].

[73] S. R. Coleman, J. Wess, and B. Zumino, Structure of phenomenological Lagrangians. 1., *Phys. Rev.* **177**, 2239 (1969).

[74] H. Song and X. Wan, A non-linear representation of general scalar extensions of the Standard Model for HEFT matching, *JHEP* **06**, 021, arXiv:2412.00355 [hep-ph].

[75] H. Song, X. Wan, and J.-H. Yu, Custodial symmetry violation in scalar extensions of the standard model\*, *Chin. Phys. C* **47**, 103103 (2023), arXiv:2211.01543 [hep-ph].

[76] P. Fileviez Perez, H. H. Patel, M. J. Ramsey-Musolf, and K. Wang, Triplet Scalars and Dark Matter at the LHC, *Phys. Rev. D* **79**, 055024 (2009), arXiv:0811.3957 [hep-ph].

[77] H. H. Patel and M. J. Ramsey-Musolf, Stepping Into Electroweak Symmetry Breaking: Phase Transitions and Higgs Phenomenology, *Phys. Rev. D* **88**, 035013 (2013), arXiv:1212.5652 [hep-ph].

[78] L. Niemi, H. H. Patel, M. J. Ramsey-Musolf, T. V. I. Tenkanen, and D. J. Weir, Electroweak phase transition in the real triplet extension of the SM: Dimensional reduction, *Phys. Rev. D* **100**, 035002 (2019), arXiv:1802.10500 [hep-ph].

[79] L. Niemi, M. J. Ramsey-Musolf, T. V. I. Tenkanen, and D. J. Weir, Thermodynamics of a Two-Step Electroweak Phase Transition, *Phys. Rev. Lett.* **126**, 171802 (2021), arXiv:2005.11332 [hep-ph].

[80] G. Buchalla, O. Cata, A. Celis, and C. Krause, Standard Model Extended by a Heavy Singlet: Linear vs. Nonlinear EFT, *Nucl. Phys. B* **917**, 209 (2017), arXiv:1608.03564 [hep-ph].

[81] Y. Du, A. Dunbrack, M. J. Ramsey-Musolf, and J.-H. Yu, Type-II Seesaw Scalar Triplet Model at a 100 TeV  $pp$  Collider: Discovery and Higgs Portal Coupling Determination, *JHEP* **01**, 101, arXiv:1810.09450 [hep-ph].

[82] G. Buchalla, F. König, C. Müller-Salditt, and F. Pandler, Two-Higgs-doublet model matched to nonlinear effective theory, *Phys. Rev. D* **110**, 016015 (2024), arXiv:2312.13885 [hep-ph].

[83] S. Dawson, D. Fontes, C. Quezada-Calonge, and J. J. Sanz-Cillero, Matching the 2HDM to the HEFT and the SMEFT: Decoupling and perturbativity, *Phys. Rev. D* **108**, 055034 (2023), arXiv:2305.07689 [hep-ph].

[84] H. Song and X. Wan, Matching the real Higgs triplet extension of Standard Model to HEFT, *JHEP* **06**, 249, arXiv:2503.00707 [hep-ph].

[85] S. Dittmaier, S. Schuhmacher, and M. Stahlhofen, Integrating out heavy fields in the path integral using the background-field method: general formalism, *Eur. Phys. J. C* **81**, 826 (2021), arXiv:2102.12020 [hep-ph].

[86] S. Navas *et al.* (Particle Data Group), Review of particle physics, *Phys. Rev. D* **110**, 030001 (2024).

[87] Combined measurements of Higgs boson production and decay at  $\sqrt{s} = 13$  TeV using up to  $140 \text{ fb}^{-1}$  of data collected by the ATLAS Experiment (2025).

[88] Combined measurements and interpretations of Higgs boson production and decay at  $\sqrt{s}=13$  TeV (2025).

[89] F. Arco, D. Domenech, M. J. Herrero, and R. A. Morales, Nondecoupling effects from heavy Higgs bosons by matching 2HDM to HEFT amplitudes, *Phys. Rev. D* **108**, 095013 (2023), arXiv:2307.15693 [hep-ph].

[90] L. Lavoura and J. P. Silva, Fundamental CP violating quantities in a  $SU(2) \times U(1)$  model with many Higgs doublets, *Phys. Rev. D* **50**, 4619 (1994), arXiv:hep-ph/9404276.

[91] F. J. Botella and J. P. Silva, Jarlskog - like invariants for theories with scalars and fermions, *Phys. Rev. D* **51**, 3870 (1995), arXiv:hep-ph/9411288.

[92] G. C. Branco, L. Lavoura, and J. P. Silva, *CP Violation*, Vol. 103 (1999).

[93] D. Fontes, J. C. Romão, and J. P. Silva,  $h \rightarrow Z\gamma$  in the complex two Higgs doublet model, *JHEP* **12**, 043, arXiv:1408.2534 [hep-ph].